Geofluids (2004) **4**, 1–22

A hydrogeologic model of stratiform copper mineralization in the Midcontinent Rift System, Northern Michigan, USA

J. B. SWENSON[1], M. PERSON[2], J. P. RAFFENSPERGER[3], W. F. CANNON[4], L. G. WOODRUFF[5] AND M. E. BERNDT[6]

[1]Department of Geological Sciences and Large Lakes Observatory, University of Minnesota Duluth, 10 University Drive, Duluth, MN 55812, USA; [2]Department of Geological Sciences, Indiana University, 1001 E. 10th St., Bloomington, IN 47405, USA; [3]US Geological Survey, Water Resources Division, MD-DE-DC District, 8987, Yellow Brick Road Baltimore, MD 21237, USA; [4]United States Geological Survey, MS 954, Reston, VA 22092, USA; [5]United States Geological Survey, 2280 Woodale Drive, Mounds View, MN 55112, USA; [6]Department of Geology and Geophysics, University of Minnesota, 310 Pillsbury Dr. S.E., Minneapolis, MN 55455, USA

ABSTRACT

This paper presents a suite of two-dimensional mathematical models of basin-scale groundwater flow and heat transfer for the middle Proterozoic Midcontinent Rift System. The models were used to assess the hydrodynamic driving mechanisms responsible for main-stage stratiform copper mineralization of the basal Nonesuch Formation during the post-volcanic/pre-compressional phase of basin evolution. Results suggest that compaction of the basal aquifer (Copper Harbor Formation), in response to mechanical loading during deposition of the overlying Freda Sandstone, generated a pulse of marginward-directed, compaction-driven discharge of cupriferous brines from within the basal aquifer. The timing of this pulse is consistent with the radiometric dates for the timing of mineralization. Thinning of the basal aquifer near White Pine, Michigan, enhanced stratiform copper mineralization. Focused upward leakage of copper-laden brines into the lowermost facies of the pyrite-rich Nonesuch Formation resulted in copper sulfide mineralization in response to a change in oxidation state. Economic-grade mineralization within the White Pine ore district is a consequence of intense focusing of compaction-driven discharge, and corresponding amplification of leakage into the basal Nonesuch Formation, where the basal aquifer thins dramatically atop the Porcupine Mountains volcanic structure. Equilibrium geochemical modeling and mass-balance calculations support this conclusion. We also assessed whether topography and density-driven flow systems could have caused ore genesis at White Pine. Topography-driven flow associated with the Ottawan orogeny was discounted because it post-dates main-stage ore genesis and because recent seismic interpretations of basin inversion indicates that basin geometry would not be conductive to ore genesis. Density-driven flow systems did not produce focused discharge in the vicinity of the White Pine ore district.

Key words: Midcontinent Rift System, ore genesis, paleohydrogeology, stratiform copper deposit

Received 19 November 2002; accepted 7 May 2003

Corresponding author: Mark Person, Department of Geological Sciences, Indiana University, 1001 E. 10th St., Bloomington, IN 47405, USA.
E-mail: maperson@indiana.edu. Tel: +1 812 855 4404. Fax: +1 812 855 7899.

Geofluids (2004) **4**, 1–22

INTRODUCTION

Several models of basin-scale groundwater circulation have been proposed to explain the formation of sediment-hosted stratiform ore deposits within a variety of tectonic settings. Early workers (Sharp 1978; Cathles & Smith 1983) emphasized the role of compaction-driven brine transport in the formation of Mississippi-Valley-type ore deposits. This mechanism may dominate the subsurface flow regime in immature basins during periods of rapid subsidence and sedimentation. Bethke (1985) demonstrated that, in the absence of a structural or stratigraphic fluid-focusing mechanism, the weak discharges and small time-integrated fluid fluxes characteristic of compaction-driven groundwater circulation render this mechanism ineffective as an ore-forming agent. Garven & Freeze (1984a), Garven (1985), Garven *et al.* (1999),

and Appold & Garven (2000) suggested groundwater flow driven by water-table topography as an ideal ore-forming mechanism within mature sedimentary basins because of its ability to focus large volumes of fluid into the basin margins for long periods and thereby generate thermal and salinity anomalies. Several workers have demonstrated that variations in pore-fluid density induced by gradients in temperature or salinity can drive free convection in thick and permeable aquifers (Wood & Hewett 1984). Raffensperger & Garven (1995) invoked this phenomenon to explain unconformity-type uranium mineralization in mature rift basins. Recently, Grigorita & Brown (2001) proposed that thermal convection was responsible for copper sulfide mineralization within the White Pine ore district. Person & Garven (1994) demonstrated that, within evolving continental rift basins, all of the aforementioned fluid-impelling mechanisms may compete for control of the hydrologic system in response to spatial and temporal variations in permeability, subsidence, water-table configuration, and basal heat flow.

Economic geologists have proposed and refined a model of district-scale metal deposition that can account for many of the physical attributes common to many of sediment-hosted stratiform copper deposits (Brown 1992, 1997). However, a generic model of basin-scale cupriferous brine circulation remains elusive, and a vigorous debate continues regarding the importance of the above-mentioned fluid-impelling mechanisms (e.g. water-table topography, sediment compaction, and buoyancy). The objective of our study is to assess the relative importance of these mechanisms in the genesis of stratiform copper mineralization at the White Pine ore district, which, in many respects, forms the type locality for the overprint model of copper deposition.

Within the Lake Superior portion of the middle proterozoic midcontinent rift system, the basal facies of the Nonesuch Formation host regional-scale, low-grade stratiform copper mineralization (Fig. 1). The mineralization is of economic grade near the Porcupine Mountains of northern Michigan with an ore body located near the town of White Pine. The geologic and geochemical aspects of the White Pine ore body have been detailed in numerous studies (White & Wright 1966; Brown 1971, 1992, 1997; Mauk 1993). However, the pioneering analysis of White (1971) remains the only quantitative model to address the role of basin-scale groundwater circulation in the formation of the White Pine ore body. Using geologically plausible estimates of aquifer and confining layer permeabilities, copper concentration of the ore-forming fluid, and duration of infiltration, White (1971) constructed a self-consistent model of mineralization that addressed two potential paleohydrologic scenarios for ore genesis at White Pine: (i) basin-scale topography-driven groundwater circulation fed by meteoric recharge along the north limb of the rift; or (ii) up-dip (marginward) migration of pore fluids driven from compacting sediments in the axial section of the basin. Because of a shortage of basin-scale geologic data, White (1971) was unable to refine his model, and the fluid-impelling mechanism responsible for stratiform mineralization remained equivocal. Garven (1985) generalized the results of his seminal study on topography-driven groundwater circulation in orogenic belts to include the genesis of the White Pine ore body. Using a cross-section based on an inferred post-rift structure of the Midcontinent Rift System in the western Lake Superior region, Garven (1985) constructed a conceptual model of the topography-driven paleoflow system he envisioned as responsible for mineralization.

Recently, the geodynamic evolution of the Midcontinent Rift System has been constrained by new basin-scale geophysical studies and high-resolution chronostratigraphy. In addition, recent exhaustive studies of the geology and geochemistry of the White Pine ore body have resolved the temperature and timing of mineralization. We have integrated this geologic information into a suite of basin-scale mathematical models of deep groundwater circulation and heat transfer in the Midcontinent Rift System and, in an extension of White's (1971) study, attempted to resolve uncertainties surrounding the fluid-impelling mechanism responsible for the basin-scale transport of ore-forming fluids to the White Pine district. We also employ equilibrium geochemical modeling and first-order mass-balance calculations to constrain the copper concentration of the ore-forming pore fluids.

GEOLOGIC SETTING

The Midcontinent Rift System is a 2200-km-long segmented continental rift (Fig. 1) of Keweenawan age (approximately 1.1 Ga) that extends as an arcuate belt from central Kansas, north through the Lake Superior region, and south-easterly to Ohio where it terminates within the Grenville Front tectonic zone (Van Schmus 1992; Cannon 1994; Hinze *et al.* 1997). The two-stage rift-filling sequence consists of a thick syn-rift volcanic package overlain by post-rift clastic sediments. Exposures of the sequence are limited to the Lake Superior region where they form the lithostratigraphic Keweenawan Supergroup (Fig. 2). Elsewhere, the existence of the rift is inferred from magnetic and gravity anomalies and limited deep-well data (Morey 1974; Witzke 1990; Allen 1994; Allen *et al.* 1997). Cannon (1994) ascribes rift failure to north-west-directed compressional stresses of the Ottawan (1090–1030 Ma) orogeny. Allen (1994) and Hinze *et al.* (1997) provide detailed and current reviews of Midcontinent Rift System geology.

The Lake Superior basin (Fig. 1) of the Midcontinent Rift System contains a broad (approximately 150 km) rift-filling sequence that reaches a thickness of approximately 30 km

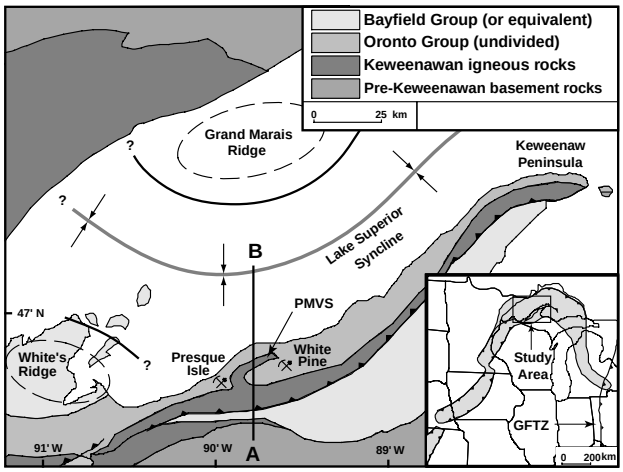

Fig. 1. Generalized geologic map of the western Lake Superior region of the Midcontinent Rift System showing model transect (A–B) and locations of stratiform ore bodies at White Pine and Presque Isle. Dashed lines indicate buried pre-Keweenawan structures; corresponding bold lines delineate the pinch-out of lower Oronto Group strata against these features. Inset: sketch of Midcontinent Rift System showing the Grenville Front tectonic zone. The light gray area in the center of the basin denotes the position of Lake Superior where no outcrop data is available.

(Cannon *et al.* 1989). Its structure and stratigraphy are constrained by interpretations of basin-scale seismic reflection data and by detailed potential-field modeling (Cannon *et al.* 1989; Allen 1994; Allen *et al.* 1997). In cross-section, the rift-filling sequence forms a broad basin with little evidence of large-scale growth faulting (Cannon 1992; Allen 1994; Allen *et al.* 1997). Allen (1994) suggests that the evolution of the western region of the Lake Superior basin was strongly influenced by two prominent crustal blocks, the Grand Marais and White's ridges (Fig. 1) that are associated with pronounced gravity anomalies and thinning of the basin fill. The thickest portion of the basin fill is delineated by the Lake Superior syncline, which coincides with the axis of Lake Superior east of Houghton, Michigan. North of the White Pine region, the syncline axis is deflected to the north-west between the Grand Marais and White's ridges and apparently terminates near Tofte, Minnesota (Allen 1994; Allen *et al.* 1997).

The post-volcanic sedimentary rocks of the Lake Superior basin form the Keweenawan Supergroup (Fig. 2), which consists of the Oronto and Bayfield groups. The volcaniclastic Oronto Group is composed of two fluvial formations, the Copper Harbor Formation and the Freda Formation, and the intercalated strata of the Nonesuch Formation. In cross-section, the Oronto Group is symmetric about the syncline axis and possesses laterally extensive, basinward-dipping seismic reflectors that display no evidence of large-scale normal faulting or plutonism (Cannon 1992; Allen *et al.* 1997). Allen (1994) divides this group into lower and upper seismic units. Lower Oronto Group strata, which comprise the Copper Harbor and Nonesuch formations, onlap the underlying volcanics, pinch out against ancestral structures, i.e. the Grand Marais and White's ridges, and, in the vicinity of the White Pine mine, thin dramatically atop the Porcupine Mountains Volcanic Structure (Fig. 1). The upper Oronto Group, i.e. the Freda Formation, is conformable with the lower Oronto Group but rests unconformably atop both lower Keweenawan volcanics near the basin margins and the Grand Marais and White's ridges. The compositionally mature fluvial formations of the Bayfield Group overlie the

Lithostratigraphy			Model Hydrostratigraphy		Material Properties						
		Quaternary Glacial Deposits			ϕ_o	b km^{-1}	c_0	c_1	$\frac{k_x}{k_z}$	λ_s $\frac{W}{m^oC}$	ρ_s $\frac{kg}{m^3}$
		Bayfield Group	Hydro-facies	Description							
		? — ? — ?									
Keweenawan Supergroup	Oronto Group	Freda Fm.	⑤	Fluvial sandstone, siltstone, and shale	0.50	0.55	-16	10	25	2.8	2650
		Nonesuch Fm.	④	Lacustrine siltstone, shale, and minor sandstone MLFA and LFA	0.60	0.85	-20	8	100	2.2	2720
			③		0.50	0.60	-16	8	50	2.3	2750
		Copper Harbor Formation	②	Upward- and basinward-fining fluvial conglomerate, sandstone, and siltstone	0.45	0.50	-15	10	25	2.5	2800
		Volcanics	①	Permeable volcanics	0.10	0.00	-20	0	500	1.6	3300
		Pre-Keweenawan basement rocks		Impermeable volcanics and basement	Hydrogeologic					Thermal	

Fig. 2. Lake Superior basin lithostratigraphy, model hydrostratigraphy, and corresponding material properties used in the baseline numerical simulation; unit thicknesses are not to scale. Abbreviations: LFA and MLFA refer to the lacustrine facies assemblage and marginal lacustrine facies assemblage of the Nonesuch Formation. The variables listed in this figure are defined in Table 1.

Oronto Group, although the nature of the contact is unclear (Daniels 1982). Allen (1994) suggests that the Bayfield Group is very thin or absent across most of the Lake Superior basin and attains an appreciable thickness only outboard of major bounding thrust faults, e.g. the Keweenaw Fault of Fig. 1.

The Copper Harbor Formation is conformable with the underlying volcanic sequence. This redbed (hematitic) formation, which attains a thickness of approximately 2 km near the syncline axis, is interpreted as an upward- and basinward-fining fluvial formation derived from lower Keweenawan volcanics (Wolff & Huber 1973; Daniels 1982; Elmore 1984; Davis & Paces 1990). The predominance of coarse- to medium-grained facies in outcrops likely reflects the proximity of these exposures to their source terranes; deep-well data from correlative formations in Midcontinent Rift System subbasins of Iowa suggest that distal (axial) sections of the Copper Harbor Formation are dominated by fine-grained facies (Witzke 1990; Anderson 1997).

The siltstone, shale, and minor sandstone of the Nonesuch Formation conformably overlie and interfinger with the Copper Harbor Formation and record a basin-scale transgressive event. The base of the Nonesuch Formation consists of a pair of meter-scale sandstone-siltstone-shale sequences, which Elmore *et al.* (1989) termed the marginal lacustrine facies assemblage. The Nonesuch marginal lacustrine facies assemblage separates the underlying sediments from the bulk of the Nonesuch Formation, which consists of 40–300 m of anoxic pyritic shale and siltstone in the lacustrine facies assemblage (Elmore *et al.* 1989). We envision the Nonesuch marginal lacustrine facies assemblage as a sedimentological transition zone that separates the coarse-grained redbeds of the Copper Harbor Formation from the fine-grained, reduced strata of the lacustrine facies assemblage. The entire formation thickens basinward and is both laterally pervasive and lenticular in shape along its apparent strike (Daniels 1982; Suszek 1997). On the basis of its stratigraphic association with fluvial formations, the Nonesuch Formation is assigned a lacustrine origin, although some researchers suggest it was deposited in a marine environment (Hieshima & Pratt 1991).

A gradational contact separates the oxidized strata of the progradational Freda Formation from the underlying lacustrine/marine facies assemblage of the Nonesuch Formation. The Freda Formation attains a maximum thickness of approximately 4 km near the syncline axis. In outcrop, it consists of a succession of meter-scale fining-upward sequences of sandstone, siltstone and shale characteristic of deposition in a meandering fluvial environment (Daniels 1982).

These structural and stratigraphic characteristics, combined with high-precision chronostratigraphy (Davis & Sutcliffe 1985; Palmer & Davis 1987; Davis & Paces 1990), suggest a four-phase model of rift evolution in the Lake Superior basin: (i) a 16-Myr period (1109–1093 Ma) of active rifting characterized by rapid extension (approximately 80 km) and the emplacement of approximately 20 km of volcanics in depocenters along the Lake Superior syncline axis; (ii) an abrupt cessation of extension, waning of volcanism, local isostasy, and immature clastic sedimentation (lower Oronto Group); (iii) a transition to regional isostasy and deposition of the Freda Formation (upper Oronto Group); and (iv) mature clastic sedimentation (Bayfield Group) in a broad flexural basin, later accompanied by regional compression (1070–1050 Ma) and partial inversion (thrusting) of the rift-filling sequence along major reverse faults (Bornhorst *et al.* 1988; Cannon 1992; Ohr 1993; Allen 1994; Allen *et al.* 1997; Bornhorst 1997).

MINERALIZATION

Native copper and copper sulfide deposits are situated along the southern margin of the Lake Superior basin, where reverse motion along the Keweenaw fault juxtaposed rift-filling volcanics and Oronto Group formations with Bayfield-Group-equivalent formations (Fig. 1). Regional-scale, low-grade stratiform copper mineralization of the basal Nonesuch Formation extends for approximately 150 km south-east of Houghton, Michigan (Mauk 1993), within which economic-grade ore bodies are located along the west (Presque Isle) and east (White Pine) flanks of the Porcupine Mountains volcanic structure. The White Pine ore body consisted of a laterally extensive (approximately 50 km^2), peneconformable cupriferous zone within the marginal lacustrine facies assemblage of the Nonesuch Formation (Fig. 3). Economic

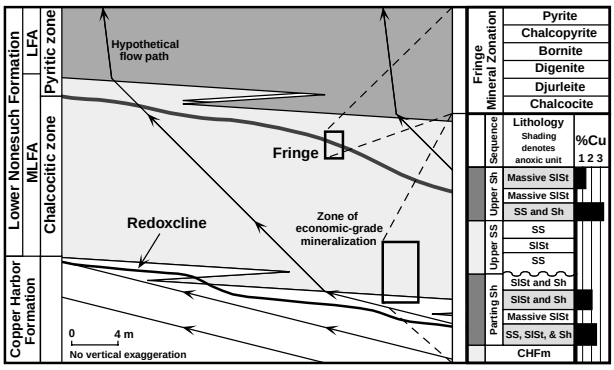

Fig. 3. Conceptual diagram of up-dip (marginward) cupriferous brine migration within the Copper Harbor Formation (CHF) and associated leakage into the marginal lacustrine facies assemblage and lacustrine facies assemblage of the superjacent Nonesuch Formation. Economic-grade mineralization is restricted to anoxic strata within the basal 5 m of the Nonesuch marginal lacustrine facies assemblage. Note that to a first order, the redoxcline corresponds to the Copper Harbor Formation/Nonesuch marginal lacustrine facies assemblage contact. Lower inset: lithostratigraphy and copper concentration of the ore-hosting basal Nonesuch marginal lacustrine facies assemblage; modified from Mauk *et al*. (1992). Abbreviations: SS, sandstone; SlSt, siltstone; and Sh, shale. Upper inset: fringe mineralization after Brown (1971).

mineralization is restricted to the basal 5 m of the marginal lacustrine facies assemblage, which consists of two transgressive sequences separated by an erosional surface. The chemically reduced siltstone and shale units within these sequences contain 2–4 wt.% copper as fine-grained disseminated chalcocite and minor native copper. The vertically averaged ore grade was 1.1 wt.% copper or approximately 30 kg Cu m^{-3} rock (Mauk 1993). The upper limit of the cupriferous zone is demarcated by a peneconformable, cm-scale transition zone (fringe) of copper–iron sulfides, ranging from chalcocite (Cu_2S) through pyrite (FeS_2), that has been interpreted as the final position of an upward advancing mineralization front (Brown 1971).

Early models for White Pine ore formation were ambiguous (White & Wright 1954; Sales 1959). The generally accepted model of mineralization (Brown 1992) invokes influx, via infiltration and/or diffusion of warm (<100°C) copper bearing, oxidizing brines from the subjacent redbeds of the Copper Harbor Formation aquifer (Fig. 3). In this model, the sulfur-rich, reduced strata of the Nonesuch Formation's marginal lacustrine facies assemblage formed a chemical sink for the copper transported in aqueous copper chloride complexes. Numerous stratigraphic and mineralogical relations within the White Pine ore body constrain the relative timing of mineralization to be coeval with diagenesis, i.e. with compaction of the formation (Mauk 1993) and high-precision radiometric dates (1081± Ma) from carbonates within the mine strata support this interpretation (Ohr 1993). A diverse suite of paleothermometers within the formation preserves a maximum temperature of approximately 130°C (Mauk 1993; Price & McDowell 1993; Price *et al.* 1996). This inferred timing of main-stage ore deposition occurred during active rifting and prior to compressional tectonism in the region. This rules out the possibility of ore formation induced by a regional topography-driven ground water flow system or by thermal convection associated with the emplacement of the Porcupine Mountains Volcanic Structure.

A second influx of cupriferous brines, coeval with the regional compression and associated structural deformation of the aforementioned four-phase model's final stage, mineralized reverse faults and adjacent strata in tectonically disturbed portions of the White Pine district with additional native copper and chalcocite. This mineralizing event postdated stratiform mineralization by 20–30 Ma (White 1968; Bornhorst *et al.* 1988; Ohr 1993) and was linked genetically to the volcanic-hosted native copper mineralization of the Keweenaw district 100 km to the north-east (Mauk *et al.* 1992).

MODELING APPROACH

We constructed two-dimensional mathematical models of basin-scale groundwater flow and heat transfer to assess the importance of several fluid-impelling mechanisms in stratiform copper mineralization of the basal Nonesuch Formation during the post-volcanic/pre-compressional phase of Lake Superior basin evolution. We applied the model to north–south cross-sections through the Lake Superior syncline including a section A–B that transects the White Pine ore district (Fig. 1). We first constructed a baseline model from a geologically reasonable set of hydrologic and thermal material properties and boundary conditions. We then performed a sensitivity study in which some of these material properties and boundary conditions were systematically varied about their baseline values and the resultant impact on the paleoflow field was quantified and interpreted. Finally, we combined the results of equilibrium geochemical modeling with simple mass-balance calculations, based on computed fluid fluxes, to constrain the copper concentration of pore fluids responsible for formation of the White Pine ore body. The mathematical model is described in an appendix to this paper.

MODEL HYDROSTRATIGRAPHY AND BOUNDARY CONDITIONS

Late Proterozoic and Phanerozoic erosion, including repeated glacial scouring in the Pleistocene, has obliterated the original surface expression of the Keweenawan Province and the tectonic quiescence that so effectively preserved the rift-filling sequence has rendered vast volumes of rock inaccessible to direct investigation. Therefore, we must cautiously infer model hydrostratigraphy and boundary conditions.

Our solution domain consists of the entire Oronto Group and the underlying uppermost volcanic section, which we subdivide into five hydrofacies (Figs 2 and 4A) that are broadly correlative with observed lithofacies. We include a volcanic hydrofacies to assess the effects of a permeable basement on the paleoflow field. The model hydrofacies were assigned representative bulk hydrologic properties on the basis of observed lithologies (Corbet & Bethke 1992). This was done because few permeability and porosity data are available for the Midcontinent Rift. Core permeability data measured from oil wells are probably not representative of conditions 1.1 billion years ago. We treat the Nonesuch marginal lacustrine facies assemblage as a hydrologic 'boundary layer' and assign it a permeability intermediate to that of the subjacent aquifer (Copper Harbor Formation) and superjacent aquitard (lacustrine facies assemblage). We construct a subsidence profile from a composite cross-section (GLIMPCE Line C and Grant-Norpac, Inc., Lines 8, 43, and 57) and high-resolution chronostratigraphy (Cannon *et al.* 1989; Davis & Paces 1990; Cannon 1992; Ohr 1993; Allen 1994; Allen *et al.* 1997; Zartman *et al.* 1997). To reduce computational requirements, we exploit the first-order symmetry of the Oronto Group and represent only

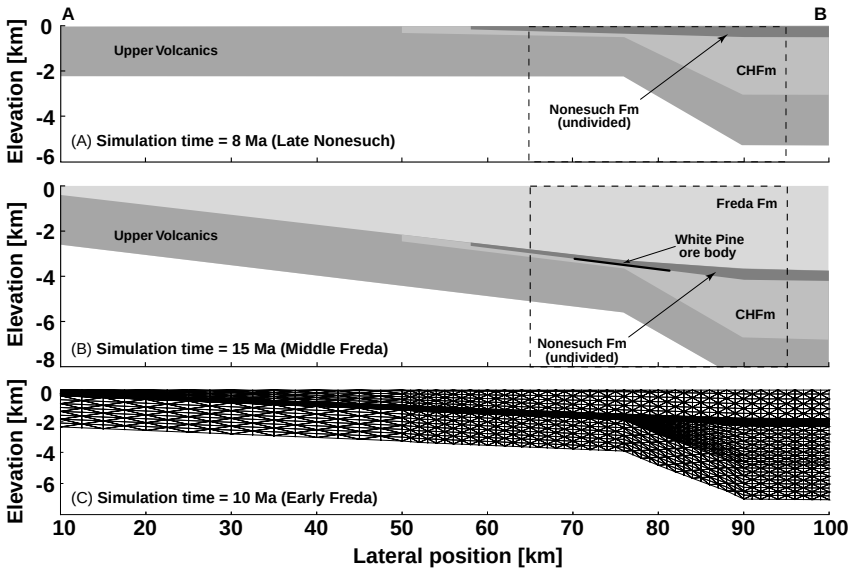

Fig. 4. (A) Model hydrostratigraphy after 8 (A) and 15 (B) million years. (C) Finite element mesh after 10 million years.

the southern limb of the syncline; the syncline axis thus forms the northern boundary of the model cross-section.

We impose a mixture of Dirichlet and Neumann boundary conditions on the governing equations for fluid flow, heat transfer, and sediment consolidation. We specify the hydraulic head (equal to the elevation of the top node in each nodal column) and temperature (10°C) along the top of the basin and a uniform heat flux across the impermeable base of the solution domain. The vertical boundaries at the basin margin and syncline axis are thermally insulated and hydraulically impermeable. We assume the water table forms a subdued replica of the surface topography (Tóth 1963). Blair (1987) and Duffy & Al-Hassan (1988) suggested that, to a first order, the surface topography of alluvial basins decays exponentially with distance from the sediment source in extensional environments. We represented the fluvial surface topography of the Lake Superior basin in this manner. We represented the denudation of sediment source terrain and the transgression/regression of the shoreline by allowing the water-table elevation, which had an exponential geometry (flat in the center of the basin and rising towards the basin margins), to decline during basin evolution. Finally, we specify a tectonic subsidence rate along the base of the solution domain.

We assume that pore-fluid salinity increases linearly with depth, attains a maximum value of 20 equivalent-wt.% NaCl at a depth of 4 km, and remains constant below this depth. We justify this approach by noting that: (i) Hanor (1987) described a similar linear relationship between salinity and depth; and (ii) residual pore fluids in the Nonesuch Formation at the White Pine mine possess salinities of approximately 20 equivalent-wt.% NaCl (Johnson *et al.* 1995). We do not allow feedback between the flow field and the distribution of salinity. Thus, the increase in salinity with depth impedes vertical flow, but the flow field does not modify salinity patterns. While this assumption only grossly approximates the actual effects of variable-density flow because of salinity, the boundary conditions for brine migration and sources of salinity within the depocenter of the Midcontinent Rift are not well known. Garven & Freeze (1984b) first implemented this approach.

MODEL RESULTS

We begin with an analysis of our baseline simulation, which used the hydrostratigraphy and material properties shown in Figs 2 and 4, a subsidence rate based on the aforementioned chronostratigraphic data (about 1 mm year^{-1}; Davis & Paces 1990; Ohr 1993) and a basal heat flux of 60 mW m^{-2}, which is consistent with paleothermometers in the Nonesuch Formation (Mauk 1993; Price & McDowell 1993; Price *et al.* 1996). While geodynamic models of rift basin evolution (e.g. McKenzie 1978; Person & Garven 1994) suggest that higher heat flow values should occur during the onset of basin formation, imposing higher heat flow values resulted in computed temperatures in the White Pine region, which were not consistent with paleo-heat-flow studies referenced above. On the basis of these results, we propose a model of stratiform mineralization at White Pine in which cupriferous brines are driven up-dip within the compacting Copper Harbor Formation and leak into the overlying Nonesuch marginal lacustrine facies assemblage, where copper is precipitated in response to a change in redox conditions of the host rocks. We then assess the sensitivity of our model to the permeability structure and the rate of Freda Formation deposition. We conclude this section with a discussion of the potential role of buoyancy-driven groundwater circulation in ore genesis at White Pine.

Baseline simulation

Our baseline model results using the parameters listed in Fig. 2 suggest that the post-volcanic hydrodynamic evolution of the Lake Superior basin was characterized by the simultaneous development of two distinct flow systems of opposite orientation. The model output is summarized graphically in Figs 5 and 6, in which we superpose contoured hydraulic head (Fig. 5) and discharge vectors and isotherms (Fig. 6) atop the model hydrostratigraphy at three stages of Oronto Group deposition.

In the early phase of post-volcanic basin evolution, a vigorous ($q_x \cong 1\ \mathrm{m\,a^{-1}}$), basinward-directed shallow flow system was established in the hydrofacies fed by meteoric recharge along the rift flanks and discharging near the syncline axis, i.e. Figs 5(A) and 6(A). Note that most discharge occurs between 90 and 100 km along the section, which is not shown in these figures. The thinning of the Copper Harbor Formation atop the Porcupine Mountains volcanic structure in the vicinity of the White Pine ore district attenuated this flow system and prevented deep, basinward groundwater circulation. This behaviour is evident in Figs 5(A) and 6(A), which depict a spatial decay in the lateral hydraulic gradient and in the magnitude of the discharge vectors basinward of the ore district. Note that the lengths of discharge vectors in the shallow, topography-driven flow system are uniform, whereas the lengths of the discharge vectors in the compaction-driven flow system scale with the flow rate. In this way both flow systems, which have very different flow rates, can be represented in a single plot. A reference vector is provided for scale. Throughout basin-scale transgression and deposition of the Nonesuch Formation, this basinward-directed, topography-driven flow system persisted within the Nonesuch Formation's time-equivalent fluvial facies, which were restricted to the basin margins. Note that during this phase of basin evolution, the Nonesuch Formation's sedimentation rate was insufficient to induce significant compaction of the axial Copper Harbor Formation, which thereby rendered the basal aquifer essentially stagnant.

During the ensuing regression and deposition of the Freda Formation, the transgressive sequence, i.e. the Nonesuch Formation, exerted a first-order control on the basin's hydrodynamic evolution by partitioning the paleoflow regime into two flow systems with opposing orientations. The basinward-

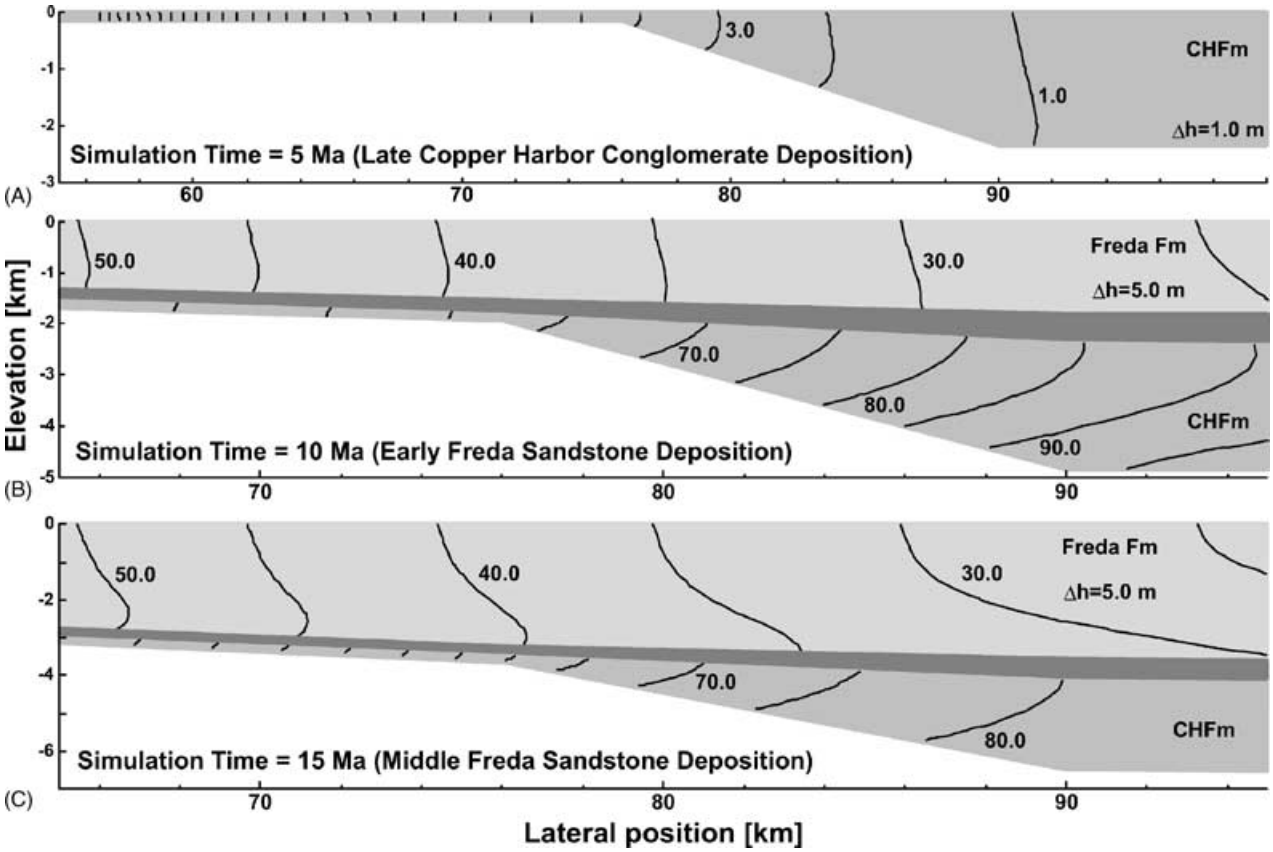

Fig. 5. Contoured hydraulic head (m) at (A) 5 Ma, (B) 10 Ma, and (C) 15 Ma of simulation time. In (A), the contour interval, Δh, is 1 m; in (B) and (C), $\Delta h = 5.0$ m. The contour intervals within the moderately overpressured Nonesuch Formation (100–300 m excess hydraulic head) are omitted for clarity.

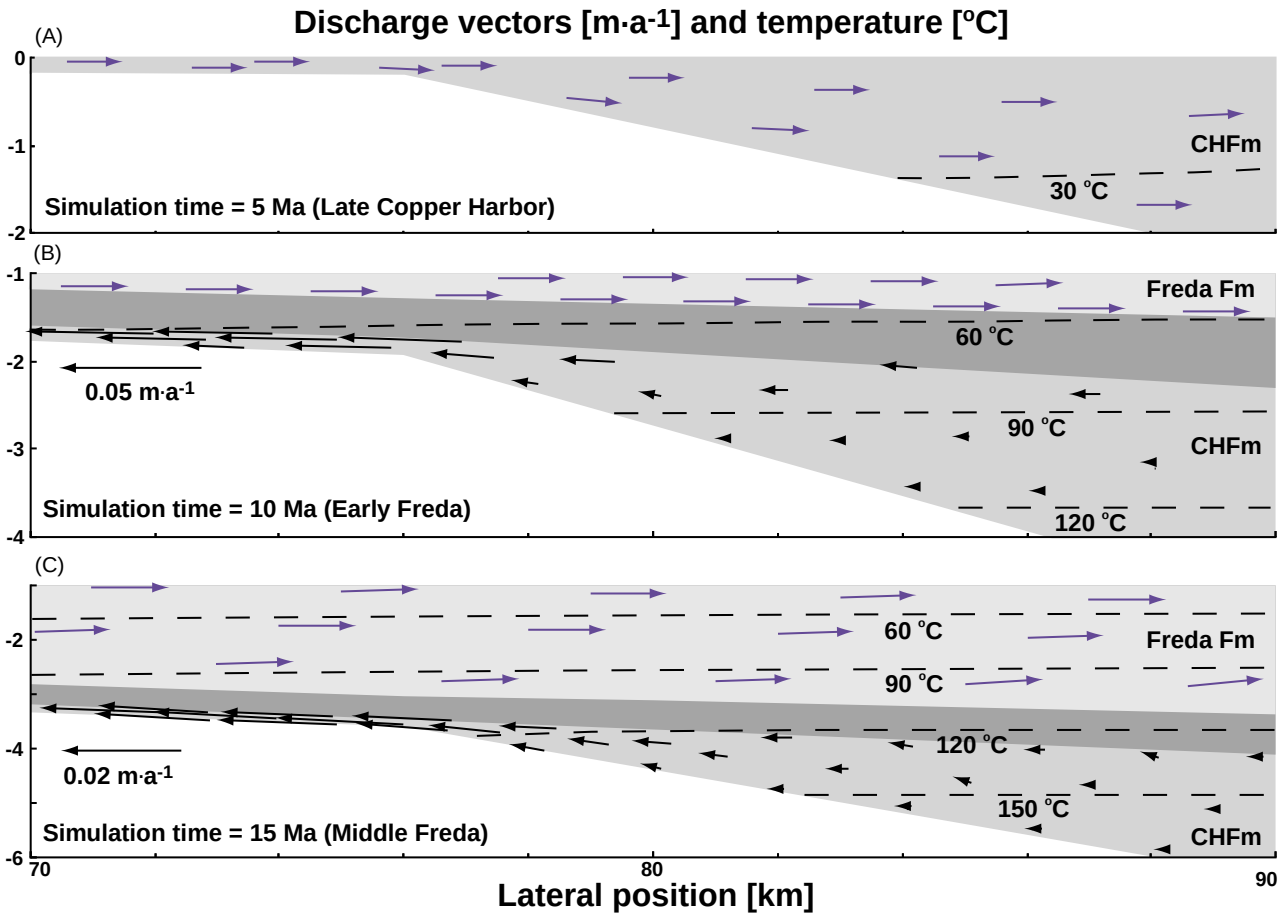

Fig. 6. Groundwater discharge vectors (m a^{-1}) and contoured temperature (°C) at (A) 5 Ma (B) 10 Ma, and (C) 15 Ma of simulation time; compare with Fig. 5. The lengths of discharge vectors in the basinward-directed topography-driven flow system are magnitude-independent, i.e. uniform and denoted with filled arrowheads. This flow system is hosted by the Copper Harbor Foramation in (A) and the Freda Formation in (B) and (C). The lengths of discharge vectors in the marginward-directed, compaction-driven flow system are magnitude-dependent, i.e. nonuniform, and denoted with open arrowheads. A reference vector is provided for scale. This flow system is hosted by the Copper Harbor Formation compacting hydrofacies in (B) and (C). Note the intense convergence of compaction-driven discharge within the near the present-day White Pine ore district. Discharge vectors within the Nonesuch Formation's lacustrine facies assemblage are not plotted. The temperature contour interval is 30°C in all figures. Note that the thermal structure is dominated by conductive heat transfer. Abbreviations: CHF, Copper Harbor Formation; MLFA, marginal lacustrine facies assemblage.

directed, topography-driven flow system was maintained in the upper aquifer, i.e. in the Freda Formation. In contrast, a marginward-directed flow system was established in the compacting basal confining unit aquifer system, i.e. in the Nonesuch Shale and underlying Copper Harbor Formation, in response to loading by the overlying Upper Nonesuch and Freda Formations.

The sedimentation rate associated with deposition of the Freda Formation was sufficient to generate moderate overpressure (100–300 m of excess head) in the axial region of the Nonesuch Formation. However, the relatively high permeability of the Copper Harbor Formation prevented the development of significant overpressure in the Copper Harbor Formation, and, as a consequence, the compaction-driven flow system in the basal aquifer was characterized not only by a weak hydraulic gradient but also by relatively vigorous lateral discharge (q_x of approximately 10^{-2} m a^{-1}). To facilitate the visualization of contoured hydraulic head in the upper and lower aquifers shown in Fig. 5(B,C), we omit contour intervals in the overpressured Nonesuch Formation and use a finer contour interval in the Copper Harbor Formation to capture the weak hydraulic gradient.

Not surprisingly, our model results indicate that conductive heat transfer dominated the thermal history of the Lake Superior basin during Oronto Group deposition. The subhorizontal orientation of the isotherms shown in Fig. 6 suggests that topography-driven groundwater circulation was too shallow and compaction-driven vertical flow was insufficient in magnitude to perturb the conductive thermal profile. Vigorous, topography-driven groundwater circulation was restricted to the relatively thin, shallow, fluvial facies near the basin margins and thus was incapable of generating

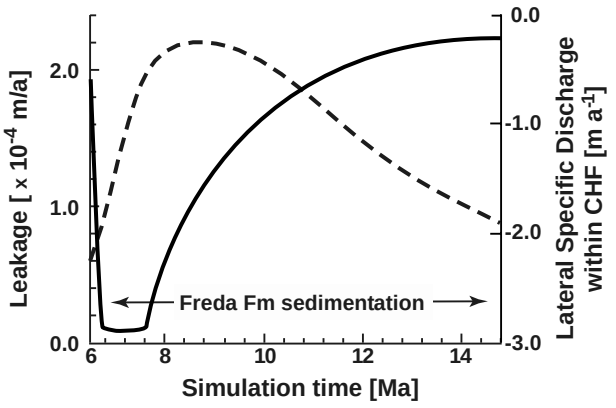

Fig. 7. Temporal evolution of compaction-driven discharge within the present-day White Pine ore district. The bold curve is computed leakage across the Copper Harbor Formation/Nonesuch marginal lacustrine facies assemblage contact (redoxcline). Abbreviations: CHF and MFLA refer to the Copper Harbor Formation and the marginal lacustrine facies assemblage of the Nonesuch Formation. The variables listed in this figure are defined in Table 1.

thermal anomalies in the axial region of the basin. Similarly, marginward-directed, compaction-driven discharge within the basal aquifer could not disrupt the conductive thermal profile. This is because groundwater velocities are too low (in the order of the sedimentation rates) within compaction-driven flow systems (Bethke 1985). Our thermal modeling suggests that paleothermometers within the White Pine ore district should reflect this conductive thermal signature.

Figure 7 shows the time evolution of compaction-driven vertical leakage across the Nonesuch marginal lacustrine facies assemblage at the White Pine ore district. Leakage attained a maximum value of approximately $2 \times 10^{-4}\,\mathrm{m\,a^{-1}}$ after approximately 3 Myr of Freda Formation deposition, which began 5.5 Myr into the simulation, before decaying quasi-exponentially throughout the remainder of sedimentation. The timing of this pulse of compaction-driven discharge within the Nonesuch marginal lacustrine facies assemblage is consistent with the inferred diagenetic timing of ore genesis at the White Pine mine (Mauk *et al.* 1992; Ohr 1993). We therefore propose that stratiform copper mineralization of the basal Nonesuch Formation can be attributed to the marginward migration of cupriferous brines within the compacting fluids leaked into and through the Nonesuch marginal lacustrine facies assemblage throughout deposition of the Freda Formation.

To test the validity of this hypothesis, we (i) quantified the volume of compaction-driven flow that percolated through the ore-hosting Nonesuch marginal lacustrine facies assemblage and (ii) demonstrated that the position of peak compaction-driven flow within the marginal lacustrine facies assemblage coincides spatially with the location of the ore district. To quantify the spatial distribution of compaction-driven discharge within the Nonesuch marginal lacustrine facies assemblage, we calculated the fluid–rock ratio and the time-integrated leakage, which we denote by χ and Q_z, respectively. The fluid–rock ratio (χ) is the ratio of time-integrated pore-fluid volumetric discharge to solid-phase volume in a unit volume (V_z) of rock. We define a fluid–rock ratio for the ore-hosting marginal lacustrine facies assemblage as:

$$\chi = \frac{1}{V_{\mathrm{u}}(1-\phi_{\mathrm{r}})}\int_0^t (|q_x| + |q_z|)\mathrm{d}t' \tag{1}$$

where ϕ_{r} is a representative porosity for the Nonesuch marginal lacustrine facies assemblage during its compaction and the unit volume symbol, V_{u}, preserves dimensional consistency ($V_{\mathrm{u}} = 1\,\mathrm{m}^3$). Relative to the coordinate system, marginward-directed compaction-driven discharge, q_z, is a negative quantity; hence, we use its magnitude in equation 1 to guarantee that χ is a positive quantity. Equation 1 is valid for positive upward discharge within the marginal lacustrine facies assemblage. The time-integrated leakage (Q_z) across a unit area, A_{u}, of the Copper Harbor Formation/Nonesuch marginal lacustrine facies assemblage contact at any lateral position is:

$$Q_z \equiv \int_0^t q_z \mathrm{d}t' \tag{2}$$

Implicit in equations 1 and 2 is the assumption of unit width (1 m) to the model cross-section. In the calculation of χ and Q_z, time is measured from the onset of Freda Formation deposition and associated compaction of the Copper Harbor Formation.

In the limit of a large permeability contrast between the Copper Harbor Formation and Nonesuch marginal lacustrine facies assemblage hydrofacies, the vertical flow occurs across the Copper Harbor Formation/Nonesuch marginal lacustrine facies assemblage contact. There is no significant lateral component to the discharge vector within the Nonesuch marginal lacustrine facies assemblage hydrofacies (q_x of approximately 0). By equations 1 and 2, $(1-\phi_{\mathrm{r}})V_{\mathrm{u}}\chi = A_{\mathrm{u}}Q_z$, where $A_{\mathrm{u}} = 1\,\mathrm{m}^2$. However, in the White Pine ore district, the Nonesuch marginal lacustrine facies assemblage consists of interbedded sandstone, siltstone and shale (Mauk 1993), which suggests that its bulk permeability is intermediate between those of the Copper Harbor Formation and the shale-dominated lacustrine facies assemblage. Hence, it is likely that a significant lateral (bedding-parallel) component of compaction-driven discharge existed within the marginal lacustrine facies assemblage throughout the proposed mineralizing event.

We define a maximum fluid–rock ratio, χ_∞, and a maximum time-integrated leakage, $Q_{z\infty}$, as the values of χ and Q_z, respectively, in the limit of large time:

$$\chi_\infty(x) = \lim_{t\to\infty}\chi(x,t) \tag{3}$$

$$Q_{z\infty}(x) = \lim_{t\to\infty}Q_z(x,t) \tag{4}$$

In the context of our model, the limit of $t \to \infty$ corresponds to the waning of Freda Formation deposition, e.g. 25 Ma in the baseline simulation, prior to the onset of late-stage rift inversion, when compaction-driven discharge within the Copper Harbor Formation had decayed to near zero and the basal aquifer was essentially stagnant. This limit represents the completion of our proposed mineralization event.

To assess the validity of compaction-driven discharge within the Copper Harbor Formation as an ore-forming mechanism, we analysed the magnitude and spatial distributions of $\chi_\infty(x)$ and $Q_{z\infty}(x)$ along two model cross-sections in the Lake Superior basin. The spatial distributions of χ_∞ and $Q_{z\infty}$ along the baseline model cross-section, A–B, which transects the White Pine ore district, are shown in Fig. 8(A). Both χ_∞ and $Q_{z\infty}$ change abruptly within the ore district, where the Copper Harbor Formation thins dramatically against the Porcupine Mountains volcanic structure. We attribute the pronounced maximum in asymptotic time-integrated leakage ($Q_{z\infty}$) to the intense convergence of compaction-driven discharge within the Copper Harbor Formation and the concomitant increase in leakage across the Copper Harbor Formation/Nonesuch marginal lacustrine facies assemblage contact. The asymptotic fluid–rock ratio (χ_∞) increases by an order of magnitude in a marginward direction across the ore district. We can explain the distribution of (χ_∞) by analysing the distribution of $Q_{z\infty}$. The large permeability contrast between the marginal-lacustrine- and lacustrine-facies-assemblage hydrofacies forces the majority of leakage across the contact between the Copper Harbor Formation and the Nonesuch marginal lacustrine facies assemblage to migrate laterally up-dip within the Nonesuch marginal lacustrine facies assemblage itself. Therefore, to a first order, we can envision χ_∞ (maximum fluid–rock ratio) within the region of thinning against the Porcupine Mountains Volcanics as the spatial integration of $Q_{z\infty}$:

$$V_u(1-\phi_r)\chi_\infty(x) \sim A_u \int_x^{x_0} Q_{z\infty}(x')\mathrm{d}x' \qquad (5)$$

where the upper limit of integration, x_0, is the lateral position at which the Copper Harbor Formation begins to thin

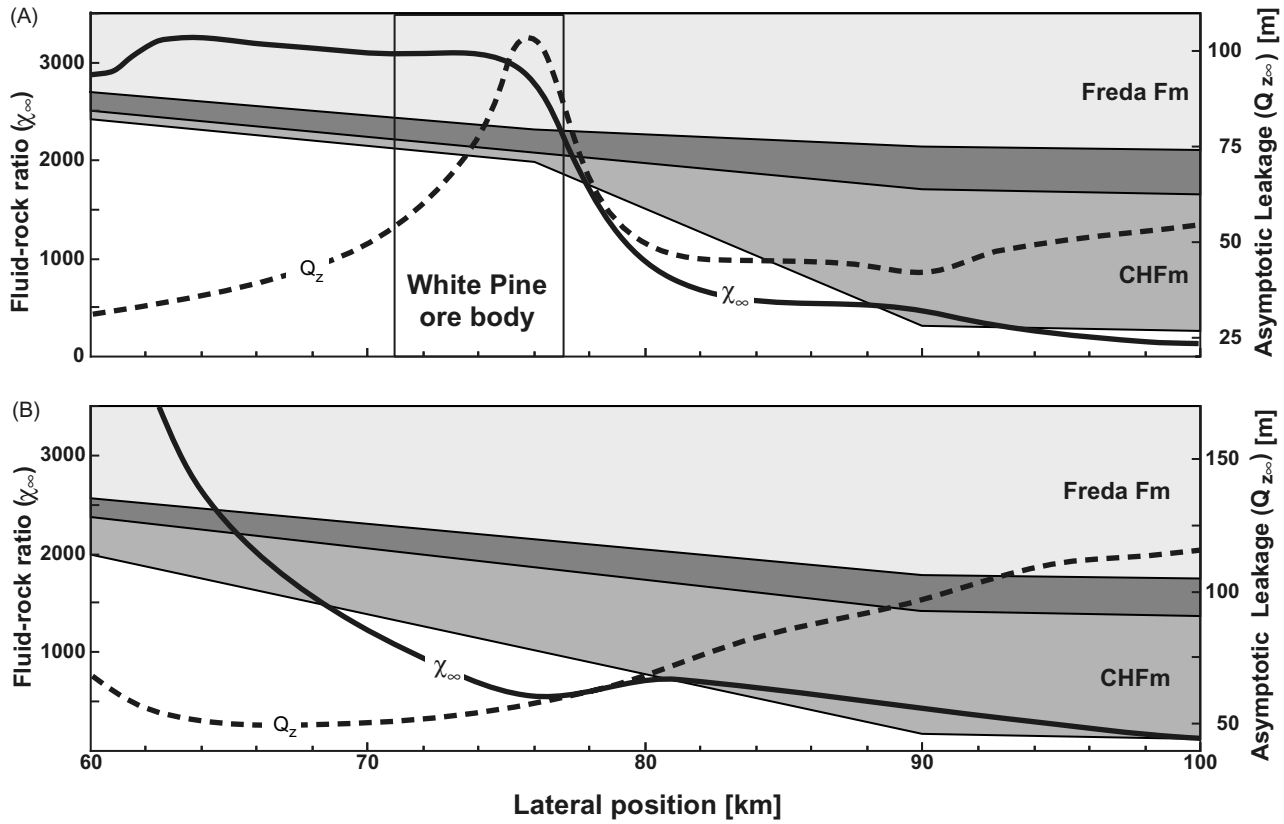

Fig. 8. (A) Spatial distributions of maximum fluid-rock ratio, $\chi_\infty(x)$, and time-integrated leakage, $Q_{z\infty}(x)$, within the Nonesuch marginal lacustrine facies assemblage hydrofacies along the model cross-section (A–B) superposed atop model hydrostratigraphy. Note the well-defined spatial maximum in $Q_{z\infty}$ is located within the present-day White Pine ore district. (B) Spatial distributions of $\chi_\infty(x)$ and $Q_{z\infty}(x)$ within the Nonesuch marginal lacustrine facies assemblage along a representative transect approximately 100 km east of the Porcupine Mountains Volcanic Structure; compare with (A). The absence of a fluid-focusing mechanism within the Copper Harbor Formation destroys the well-defined spatial maximum in $Q_{z\infty}$ that is evident in (A). Note that in both (A) and (B), solid-circle and open-circle curves denote χ_∞ $Q_{z\infty}$, respectively, and CHF denotes the Copper Harbor Formation. The variables listed in this figure are defined in Table 1.

against the Porcupine Mountains Volcanic Structure, i.e. where $\chi_\infty(x)$ displays its basinward inflection point. Again, we retain the V_u and A_u symbols to preserve dimensional consistency. The relationship of equation 5 is clearly evident in Fig. 8(A).

In our model, the White Pine ore body occupies an approximately 6-km-wide zone centered approximately 2 km marginward of the maximum in $Q_{z\infty}$, near the marginward inflection point in χ_∞ (Fig. 8A). We propose that cupriferous brines infiltrating the Nonesuch marginal lacustrine facies assemblage from the underlying Copper Harbor Formation may have migrated laterally within the permeable and oxidized sandstone and siltstone facies of ore-hosting marginal lacustrine facies assemblage for significant distances prior to encountering the reducing conditions thought to induce copper precipitation. This lateral flow component may explain the slight marginward translation of the ore body relative to the maximum in $Q_{z\infty}$. However, our model of basin-scale groundwater circulation cannot readily resolve such second-order, i.e. mine-scale, features, which would require both reaction-path modeling and detailed knowledge of the Nonesuch marginal lacustrine facies assemblage stratigraphy within the ore district.

To illustrate the importance of the Porcupine Mountains volcanic structure as a fluid-focusing mechanism in ore genesis, we constructed a second model cross-section situated approximately 100 km to the east of the Porcupine Mountains volcanic structure. The spatial distributions of χ_∞ and $Q_{z\infty}$ that we obtained with this cross-section are displayed in Fig. 8(B). The gentle marginward thinning of the Copper Harbor Formation for lateral positions less than 90 km produced a monotonic decay in $Q_{z\infty}$ and an overall monotonic increase in χ_∞. The behavior of $Q_{z\infty}$ reflects the marginward transition from vertical flow to lateral flow in the basal, compacting sediments of intracratonic basins (Bethke 1985). By equation 5, it follows that χ_∞ should increase monotonically within the hydrologic 'boundary layer' (marginal lacustrine facies assemblage) as the lateral discharge component in equation 1 increases in the marginward direction in response to the capture of additional leakage across the contact between the Copper Harbor Formation and the marginal lacustrine facies assemblage. These distributions of χ_∞ and $Q_{z\infty}$ might explain the regional, low-grade stratiform mineralization of the marginal lacustrine facies assemblage east of the White Pine region. However, in the absence of pronounced thinning of the basal aquifer and intense focusing of lateral flow, it appears that the majority of compaction-driven discharge within the Copper Harbor Formation simply escaped the basin via the Nonesuch Formation's time-equivalent fluvial facies near the basin margin. We thus conclude that the presence of a fluid-focusing structure, such as the Porcupine Mountains volcanic structure, was the dominant control on the spatial distribution of ore bodies within the basal Nonesuch Formation.

Model sensitivity to permeability structure

Our baseline model results suggest that the structural and stratigraphic architecture of the Lake Superior basin controlled the post-volcanic/pre-compressional paleoflow regime. The observed partitioning of the flow regime would be maintained for any reasonable set of bulk permeabilities assigned to the model hydrofacies. However, the permeability contrasts between the Copper Harbor Formation, the Nonesuch marginal lacustrine facies assemblage, and lacustrine facies assemblage hydrofacies likely controlled the amount and spatial distribution of compaction-driven discharge that percolated through the ore-hosting strata of the marginal lacustrine facies assemblage. As stated above, the permeability of these pre-compressional strata are poorly known and modern permeability measurements from core data are probably not representative of basin scale values (Garven 1985). To quantify the dependence of χ_∞ and $Q_{z\infty}$ on these permeability contrasts, we performed a sensitivity analysis in which the permeability contrasts between the marginal lacustrine facies assemblage hydrofacies, lacustrine facies assemblage hydrofacies, and the Copper Harbor Formation were varied systematically. To facilitate the comparison of model results, we define the following permeability contrast parameters:

$$\xi = \log(k_{CHF}/k_{MLFA}) \quad (6)$$

$$\eta = \log(k_{CHF}/k_{LFA}) \quad (7)$$

where k_{CHF}, k_{MLFA}, and k_{LFA} represent the bedding-parallel permeabilities of the subscripted hydrofacies. A value of $\xi = 2$ corresponds to a permeability contrast of 100 between the Copper Harbor Formation and the ore-hosting marginal lacustrine facies assemblage hydrofacies; likewise, a value of $\eta = 4$ corresponds to a four-order-of-magnitude permeability contrast between the Copper Harbor Formation and the lacustrine facies assemblage (bulk Nonesuch Formation) hydrofacies.

We analysed first the sensitivity of χ_∞ and $Q_{z\infty}$ to variations in the Copper Harbor Formation/Nonesuch marginal lacustrine facies assemblage bulk permeability contrast (ξ) by fixing the Copper Harbor Formation/lacustrine facies assemblage permeability contrast at the baseline value ($\eta = 4.3$) and varying the bulk permeability of the Nonesuch marginal lacustrine facies assemblage such that ξ assumed a range consistent with the lithologies of the upper Copper Harbor Formation and basal Nonesuch Formation in the White Pine mine (Mauk 1993). The results of our numerical experiment are summarized graphically in Fig. 9, which shows the spatial distributions of χ_∞ and $Q_{z\infty}$ in the vicinity of the White Pine ore district for ξ values of 1.6, 2.1, and 2.6. The gross structure of χ_∞ and $Q_{z\infty}$ is relatively insensitive to variations in the Copper Harbor Formation/Nonesuch marginal lacustrine facies assemblage bulk permeability contrast.

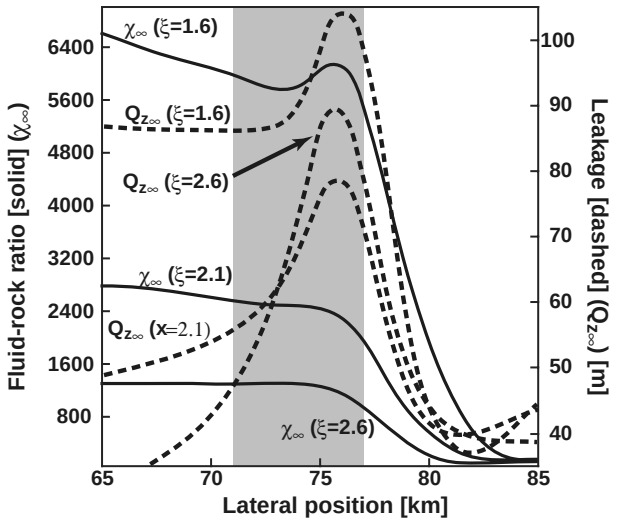

Fig. 9. Spatial distributions of χ_∞ and $Q_{z\infty}$ in the Nonesuch marginal lacustrine facies assemblage in the vicinity of the White Pine ore district for several values of the Copper Harbor Formation/Nonesuch marginal lacustrine facies assemblage bulk permeability contrast ($\xi = 1.6$, 2.1, and 2.6). Solid and dashed curves denote χ_∞ and $Q_{z\infty}$, respectively. Shaded area delineates the lateral extent of the White Pine ore body. Abbreviations: CHF, Copper Harbor Formation; MLFA, marginal lacustrine facies assemblage. The variables listed in this figure are defined in Table 1.

As the permeability contrast is increased, i.e. as ξ increases, the lateral position of the local maximum in $Q_{z\infty}$ remains nearly stationary, but the width and magnitude of the distribution decreases. The sensitivity of χ_∞ to variations in ξ is more pronounced, with the maximum value in the ore district decreasing by a factor of 4.4 ($6200 \rightarrow 1400$) as the Copper Harbor Formation/marginal lacustrine facies assemblage permeability contrast is increased by approximately an order of magnitude, from 1.6 to 2.6.

We performed a similar exercise to determine the influence of the Copper Harbor Formation/lacustrine facies assemblage bulk permeability contrast on the maximum values of χ_∞ and $Q_{z\infty}$ within the ore district. We fixed the bulk permeability of the shale-dominated lacustrine facies assemblage at its baseline value and systematically varied the bulk permeability of the Copper Harbor Formation over a range consistent with lithofacies observed in outcrop; throughout this process, we adjusted the marginal lacustrine facies assemblage bulk permeability such that ξ is approximately 2.1. The resultant spatial distributions of χ_∞ and $Q_{z\infty}$ were identical in structure to those of the intermediate data set ($\xi = 2.1$) shown in Fig. 9 for the entire range of η that we investigated. The maximum values of both χ_∞ and $Q_{z\infty}$ within the ore district, which we plot in Fig. 10, decrease monotonically with increasing η and approach asymptotic values for $\eta > 7$. Our data suggest that both χ_∞ and $Q_{z\infty}$ are relatively insensitive to variations in the Copper Harbor Formation/lacustrine facies assemblage bulk permeability contrast.

Finally, we investigated the influence of a permeable volcanic basement of the Porcupine Mountains volcanic structure on the spatial distribution of χ_∞ and $Q_{z\infty}$ by assigning the upper 2 km of the volcanic hydrofacies a bulk permeability comparable to that of the superjacent hydrofacies, i.e. k_{VOLC} of approximately $10^{-14}\,\mathrm{m}^2$. In this scenario, the Copper Harbor Formation and uppermost volcanics behaved as a composite aquifer. Thinning of this composite aquifer near the Porcupine Mountains volcanic structure was sufficient to produce a weak maximum in $Q_{z\infty}$ and an increase in χ_∞ (by equation 5) within the present-day White Pine ore district (Fig. 11). Note, however, that the value of χ_∞ within the ore district is less than that of Fig. 9 by an order of magnitude. Hence, we conclude that a permeable volcanic basement would have destroyed the intense fluid-focusing effect of the porcupine mountains volcanic structure.

On the basis of our sensitivity study, we draw the following conclusions regarding the influence of permeability structure on compaction-driven ore genesis at White Pine: (i) a significant permeability contrast between the basal aquifer (Copper Harbor Formation) and both the underlying volcanics and the overlying Nonesuch Formation (lacustrine facies assemblage) is necessary to focus lateral discharge within the compacting basal aquifer and generate sufficient flow convergence atop the porcupine mountains volcanic structure to produce a well-defined spatial maximum in $Q_{z\infty}$; (ii) a two-order-of-magnitude contrast in bulk permeability between the Copper Harbor Formation and marginal lacustrine facies assemblage (ξ of approximately 2) yields spatial distributions of χ_∞ and $Q_{z\infty}$, consistent with the location and lateral extent of the White Pine orebody; (iii) a large value of ξ generates a 'sharp' spatial maximum in $Q_{z\infty}$ but severely attenuates the maximum value of χ_∞ within the ore district; and (iv) the spatial distributions of χ_∞ and $Q_{z\infty}$ and their maximum values within the ore district are insensitive to the bulk permeability contrast between the Copper Harbor Formation and lacustrine facies assemblage (η), provided that it is large enough to satisfy condition (i).

Sensitivity to Freda Formation sedimentation rate

The duration of Freda Formation deposition is constrained by the timing of Nonesuch Formation deposition at 1085 Ma (Ohr 1993) and rift inversion at 1060 ± 20 Ma (e.g. Cannon *et al.* 1990; Cannon 1992). Our baseline simulation employs a 25-Myr period of deposition, i.e. 1085–1060 Ma. In traditional studies of compaction-driven groundwater circulation within thick sequences of impermeable sediments, the sedimentation rate exerts a first-order control on the generation of overpressure and the magnitude of groundwater discharge (Bethke 1985). To investigate the sensitivity of χ_∞ and $Q_{z\infty}$ to variations in the rate of compaction, we varied the duration of Freda Formation deposition by ± 10 Myr about the baseline value so as to encompass

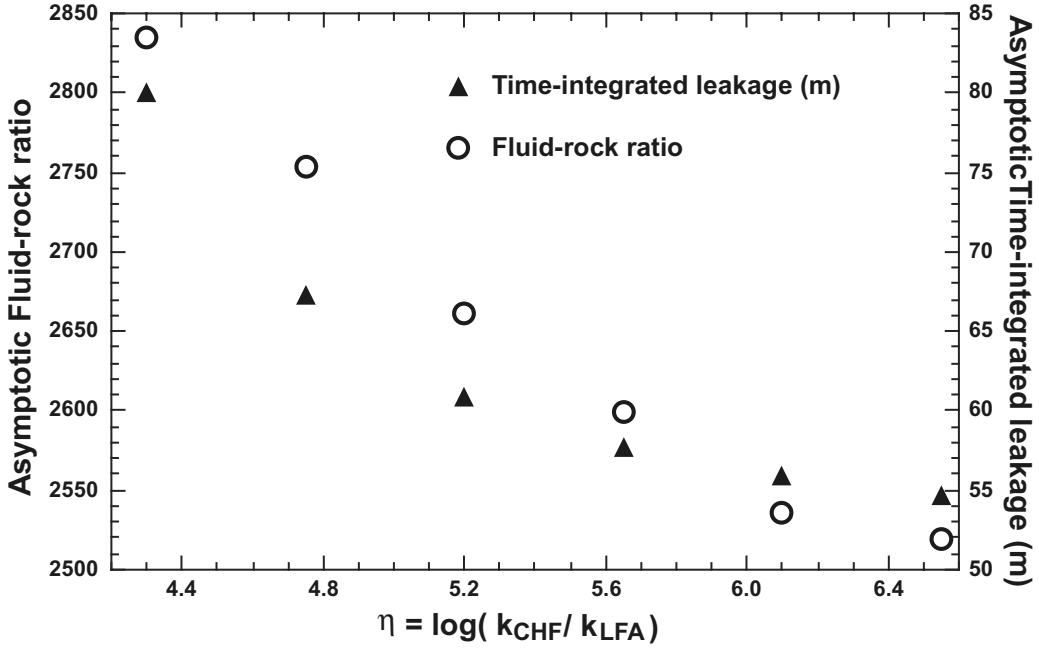

Fig. 10. Maximum values of χ_∞ and $Q_{z\infty}$ within the White Pine ore district for various values of the Copper Harbor Formation/lacustrine facies assemblage bulk permeability contrast (η). Refer to text for details. The variables listed in this Figure are defined in Table 1.

the uncertainty in the duration of rift inversion. We determined that an increased sedimentation rate amplified the magnitude and reduced the duration of the pulse of compaction-driven discharge within the Copper Harbor Formation and Nonesuch marginal lacustrine facies assemblage; conversely, a reduced sedimentation rate generated a longer-lived, lower-amplitude pulse of compaction-driven discharge. However, the maximum values of χ_∞ and $Q_{z\infty}$ within the White Pine ore district changed by less than 10% relative to the baseline results of Fig. 8(A). We therefore conclude that the leakage of compaction-driven discharge into the Nonesuch marginal lacustrine facies assemblage is insensitive to the compaction rate of the basal aquifer. This is a consequence of the efficacy with which the Nonesuch Formation's lacustrine facies assemblage impeded hydraulic communication between the underlying Copper Harbor Formation and the overlying Freda Formation ($\eta > 4$). Pore fluids in the Copper Harbor Formation are driven laterally to basin margins, regardless of the rate of aquifer compaction.

Density-driven circulation and ore genesis

Jowett (1986) ascribed the formation of the Kupferschiefer stratiform copper deposit in Poland to large-scale free convection within the basal aquifer beneath the ore-hosting transgressive sequence. Although our baseline simulation failed to generate free convection within the basal aquifer (hydrofacies), we performed a sensitivity study to investigate more thoroughly the potential for free convection to circulate cupriferous brines in the Copper Harbor Formation to

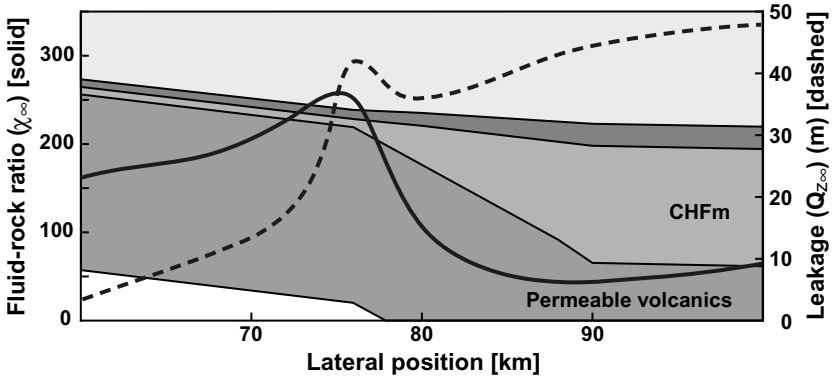

Fig. 11. Spatial distribution of $\chi_\infty(x)$ and $Q_{z\infty}(x)$ in the Nonesuch marginal lacustrine facies assemblage hydrofacies along the model transect A–B with a permeable volcanic basement. Compare with Fig. 9; note the differences in the ranges of χ_∞ and $Q_{z\infty}$ plotted in Fig. 8 and this figure. CHF denotes Copper Harbor Formation. The variables listed in this figure are defined in Table 1.

the White Pine ore district. We tested two hypotheses: (i) that stratiform mineralization was formed by free convection contemporaneous with Freda Formation deposition; and (ii) that the inferred timing of stratiform mineralization at White Pine was incorrect, and that stratiform mineralization, in fact, post-dated deposition of the Freda Formation but pre-dated rift inversion. For the latter scenario, in which compaction of the basal aquifer would have been nearly complete, we assumed that the Lake Superior basin paleoflow system was in dynamic equilibrium with its hydrologic and thermal boundary conditions, which allowed us to use a stream-function-based model of groundwater circulation and heat transfer (Evans & Raffensperger 1992).

To assess the potential for buoyancy-driven groundwater circulation within the hydrofacies during deposition of the Freda Formation, we systematically increased the basal heat flux, J_z, above its baseline value of $60\,\mathrm{mW\,m^{-2}}$ in an effort to induce free convection. We failed to observe evidence of organized free convection within the hydrofacies during its compaction for heat fluxes less than approximately $100\,\mathrm{mW\,m^{-2}}$. When we observed organized free convection, i.e. for $J_z > 100\,\mathrm{mW\,m^{-2}}$, it was restricted to the axial portion of the basin and thus was far removed from the White Pine ore district. We note that a heat flux greater than $80\,\mathrm{mW\,m^{-2}}$ is inconsistent with paleothermometers in the Nonesuch Formation (Price & McDowell 1993; Price *et al.* 1996). We therefore conclude that for all reasonable values of J_z, the compaction-driven flow system established within the hydrofacies was sufficiently strong to overwhelm free convection during deposition of the Freda Formation, which indicates that the first hypothesis posed above (White Pine stratiform copper mineralization by free convection) is false.

To test the second hypothesis, we employed the stream-function-based model of Evans & Raffensperger (1992) and varied the basal heat flux (J_z) and consolidation coefficient, b, of the hydrofacies systematically (see equations A.9–A.10 in the Appendix). For the steady-state paleoflow system, we used the modified Rayleigh-Darcy number, Ra, to quantify the tendency for organized free convection to develop in the basal aquifer

$$Ra = \frac{\alpha_T \rho_f{}^2 c_f g H \Delta T}{\mu_f (\lambda_f{}^{\phi} \lambda_s{}^{1-\phi})} \frac{k_x k_z}{[\sqrt{k_z} + \sqrt{k_z}]^2} \qquad (8)$$

where H and ΔT scale the thickness of the basal aquifer and the temperature difference across it, respectively. With b fixed at its baseline value of $0.5\,\mathrm{km^{-1}}$, we first increased J_z by as much as $40\,\mathrm{mW\,m^{-2}}$ above its baseline value but failed to observe any organized free convection. This result is consistent with the representative values of Ra for the basal aquifer, all of which were well below a reasonable range of critical values for a horizontal layer with finite conducting boundaries (Riahi 1983; Nield & Bejan 1992).

We next held J_z fixed at its baseline value and systematically decreased the value of b for the hydrofacies, which decreases the rate of compaction relative to depth of burial and effectively increases the depth at which significant compaction and resultant permeability reduction occur (by equations A.4 and A.5, respectively). Relative to the baseline value of $0.5\,\mathrm{km^{-1}}$, it was necessary to reduce b to $0.1\,\mathrm{km^{-1}}$ in order to preserve sufficient porosity and therefore permeability within the Copper Harbor Formation for free convection to develop (Figs 12 and 13). Estimated Ra values under this scenario are above critical values. Organized convection cells developed deep within the basin, and their geometry was constrained by the thickness and anisotropy of the Copper Harbor Formation as well as by the position of lateral boundaries (or effectively by thinning on the flanks of the Porcupine Mountains volcanic structure). However, we failed to observe convective circulation in the region of stratiform ore mineralization. Reducing b (the effective compressibility coefficient) to $0.1\,\mathrm{km^{-1}}$ presumes that the Copper Harbor Formation was significantly under-compacted, such that the magnitude of compaction-driven discharge would have been greatly reduced. Within the basin, it thus appears that the mechanisms of compaction- and buoyancy-driven flows are mutually exclusive. When significant compaction accompanies burial, porosity and permeability are reduced such that free convection is unlikely, while for the case of undercompaction, i.e. if b is small, free convection may develop, but groundwater circulation produced by compaction will be negligible. On the basis of the significant under-compaction required to generate free convection and the absence of convective circulation proximal to the ore district, we dismiss the second hypothesis and conclude that buoyancy-driven groundwater circulation, likely, was not the fluid-impelling mechanism for ore genesis at White Pine. Ore genesis by compaction-driven flow remains the most likely scenario to explain the occurrence of main-stage ore mineralization at White Pine.

GEOCHEMISTRY

White (1971) inferred a copper concentration of 50 p.p.m. for White Pine ore-forming fluids, and although concentrations above 10° p.p.m. have not been observed in modern low-temperature formation waters (Hanor 1979), their existence has been predicted in aqueous environments characterized by high chloride activity and oxygen fugacity (Brown 1971; Rose 1976, 1989; Barnes 1979; Jowett 1986; Sverjensky 1987). To estimate copper concentrations of connate fluids during alteration of highly oxidized volcanic rocks, we performed simulations using the EQ3/6 geochemical software package and SUPCRT92 database (Johnson *et al.* 1992; Wolery 1992), which we modified to incorporate the Cu–Cl-complex association constants from Helgeson (1969). We selected a pair of stable mineral assemblages, laumontite–paragonite–kaolinite–quartz (L–Pa–K–Q) and albite–paragonite–prehnite–quartz (A–Pa–Pr–Q), to

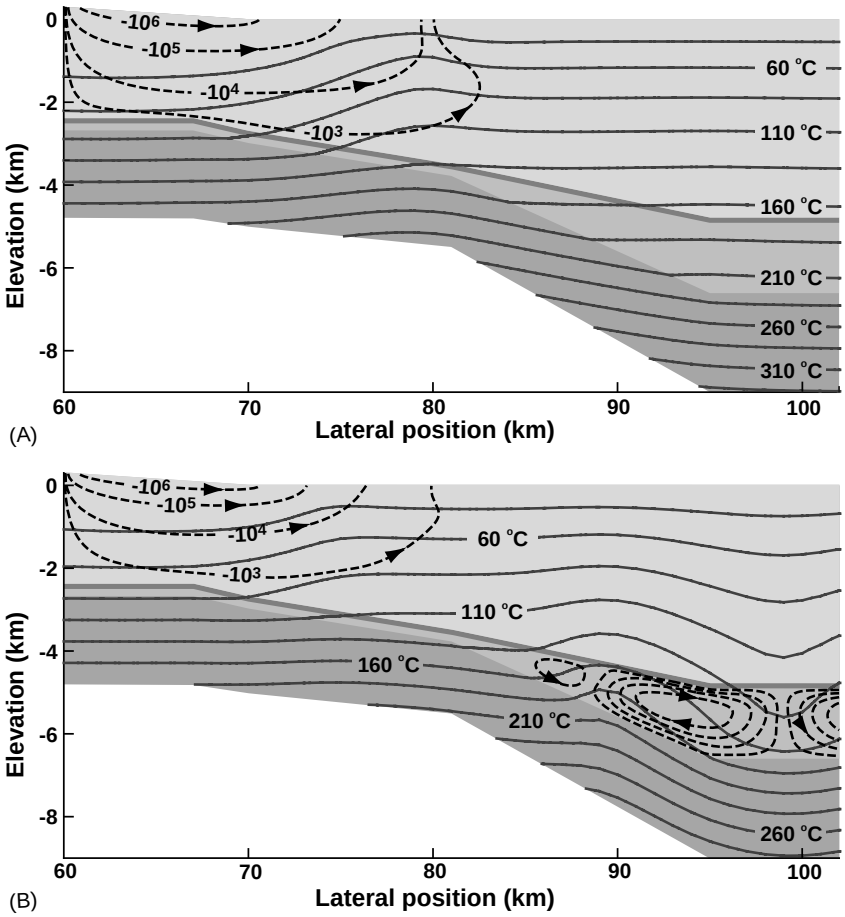

Fig. 12. Cross-sectional model representation of the Lake Superior basin paleoflow field at steady state following cessation of Freda Formation deposition and corresponding compaction of the Copper Harbor Formation: (A) using baseline material properties (Fig. 2); and (B) using a reduced value of b for the Copper Harbor Formation. Dashed lines are streamlines, or contours of the stream function, $\Psi(x,z)$ (kg m^{-2} a^{-1}). Note that the contour increment is logarithmic in the Freda Formation; the contour increment in (B) is 10^4 kg m^{-1} a^{-1}.

approximate by equilibration the chemistry of pore fluids within the oxidized volcaniclastic sediments. Oxygen fugacity, f_{O_2}, was constrained by either Cu^0–CuO or Fe_2O_3–Fe_3O_4 buffer assemblages, total chloride (ΣCl) was allowed to range between 0.5 and 1.0 M, and copper solubility at each condition was estimated from the saturation of native copper Cu^0. Redox conditions of the Copper Harbor Formation are inferred from mineralogic evidence. Both copper and iron in the Copper Harbor Formation were probably altered to cuprite (CuO) and hematite (Fe_2O_3) during fluvial transport and deposition. Butler & Burbank (1929) state that the bulk of the iron oxide in the Conglomerate is hematite, which was the result of primary weathering and oxidation. Scofield (1976) found that native copper associated with iron-bearing minerals such as titanomagetite in unaltered (nonmineralized) portions of basalt flows of the Portage Lake Volcanics. This native copper could have been entrained into the redbeds of the Copper Harbor Formation, and subsequently oxidized to cuprite.

Equilibration of pore fluids with the above assemblages over a temperature range of 50–150°C produced Na–Ca–Cl brines with Na/Ca ratios similar to those of modern formation waters (Hanor 1979) and pH values of 5.8–7.2. The temperature dependence of copper concentrations for the assemblages at several ΣCl molarities is displayed in Fig. 14; apparently, potent ore-forming brines may be generated if Cu^0–CuO is the oxygen buffer and if ΣCl is greater than that of seawater. Copper solubility is reduced by approximately four orders of magnitude. if, f_{O_2} is constrained by the Fe_2O_3–Fe_3O_4 redox buffer, Fig. 14 suggests that the presence of CuO (cuprite) in the alteration assemblage, and ΣCl molarities higher than those of seawater in the mineralizing fluid provide sufficient copper concentrations to generate an ore deposit with the low water–rock ratios (χ) characteristic of a compaction dominated system.

The paleoflow model output provides a range of hydrologically reasonable χ_∞ values within the Nonesuch marginal lacustrine facies assemblage at White Pine, and the data of Fig. 14 constrain the potential copper concentration C_{Cu} within the aquifer. The ore within the Nonesuch marginal lacustrine facies assemblage at White Pine, m_{Cu}, must satisfy the following first-order expression of mass balance:

$$m_{Cu} = \chi_\infty C_{Cu} \rho_f \varepsilon \quad (9)$$

where C_{Cu} and ρ_f are, respectively, the average copper concentration in the ore-forming fluid and the density of that fluid. The presence of a lateral flow component within the permeable, oxidized strata of the Nonesuch marginal

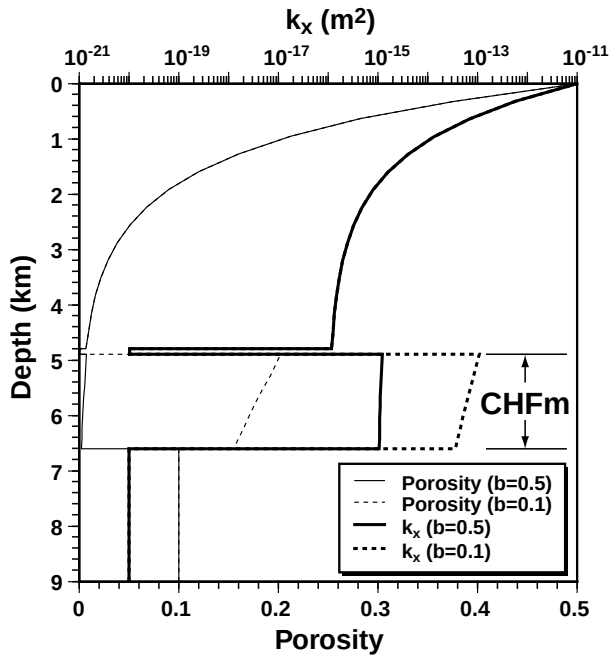

Fig. 13. Porosity-depth and permeability-depth curves for the steady-state postcompaction simulations shown in Fig. 12. The curves are for the center of the basin and for two values of *b* for the Copper Harbor Formation. CHF denotes the Copper Harbor Formation. The variables listed in this figure are defined in Table 1.

lacustrine facies assemblage introduces the possibility of lateral (up-dip) brine migration over significant distances prior to metal precipitation. Without resorting to reaction-path modeling, we can quantify this effect with a depositional efficiency, ε. In the absence of a lateral flow component within the Nonesuch marginal lacustrine facies assemblage, i.e. if $\xi \gg 1$, ε would assume a value of unity, because all dissolved copper crossing a unit area of the Copper Harbor Formation/Nonesuch marginal lacustrine facies assemblage contact would precipitate to form an ore column within the marginal lacustrine facies assemblage of height $Q_{z\infty}\rho_f C_{\mathrm{Cu}} m_{\mathrm{Cu}}{}^{-1}$, where m_{Cu} is the average ore grade. In the presence of a lateral flow component, ε quantifies the extent to which the ore-hosting marginal lacustrine facies assemblage 'filters' copper from the infiltrating brines.

We used equation 9 to generate a family of curves (Fig. 15), each member of which represents the locus of fluid–rock ratio and ore-forming fluid copper concentration pairs $(\chi_\infty, C_{\mathrm{Cu}})$ that satisfies the mass-balance constraint at White Pine, i.e. m_{Cu} approximately 30 kg Cu m^{-3} rock, for a specified depositional efficiency. The data of Fig. 15

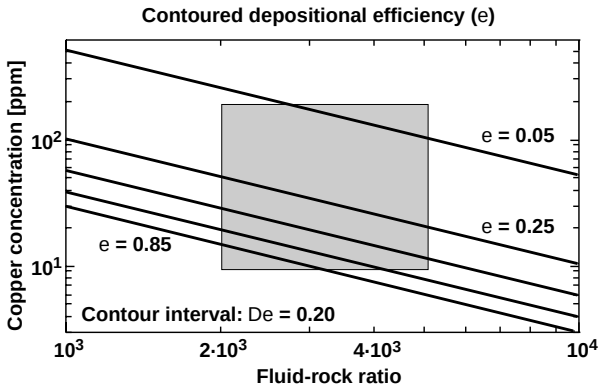

Fig. 15. Family of lines, each member of which represents the locus of fluid–rock ratio and ore-forming-fluid copper concentration pairs $(\chi_\infty, C_{\mathrm{Cu}})$ that satisfy the mass-balance constraint at White Pine (m_{Cu} of approximately 30 kg Cu m^{-3} rock) for a specified efficiency (ε) of copper deposition. The variables listed in this figure are defined in Table 1.

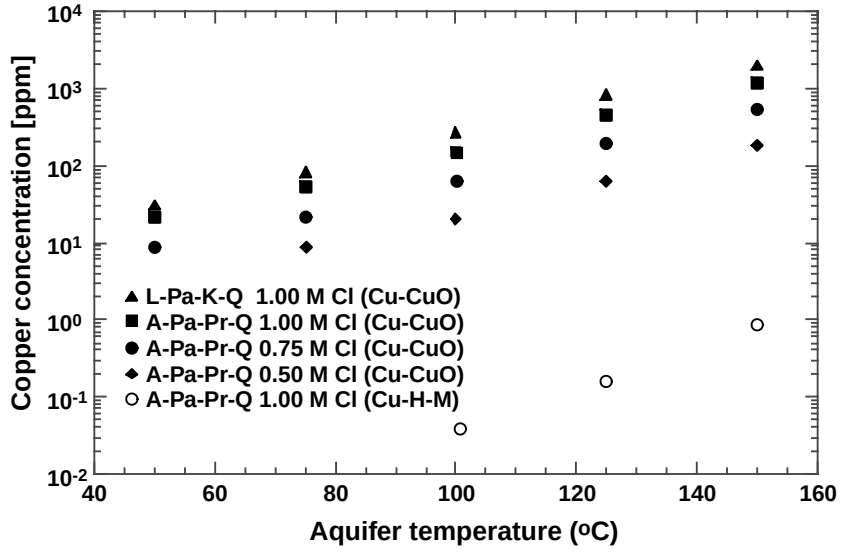

Fig. 14. Copper solubility within the chemofacies as a function of redox, temperature, and chloride concentration. Brine composition was calculated by assuming equilibration with respect to laumontite–paragonite–kaolinite–quartz (L–Pa–K–Q) or albite–paragonite–prehnite–quartz (A–Pa–Pr–Q). Total chloride (ΣCl) ranged from 0.50 to 1.00 M. Redox was controlled by native copper–cuprite (Cu–CuO) or hematite–magnetite (H–M) assemblages. Refer to text for explanation.

indicate that cupriferous brines derived from the consolidating hydrofacies could satisfy the mass-balance requirement at White Pine under a variety of reasonable hydrologic (χ_∞) and geochemical (C_{Cu}, ε) scenarios.

DISCUSSION

As the Porcupine Mountains Volcanic structure is situated between two depocenters, the Allouez and Marquette subbasins, along the Lake Superior syncline (Fig. 1), our cross-sectional models may under predict the degree of compaction-driven fluid focusing along the southern margin of this basin. The Porcupine Mountains Volcanic structure behaves like a blunt, semicircular dome in the otherwise uniform thickness Copper Harbor Conglomerate. In map view, compaction-driven discharge from each depocenter combines to yield a more or less uniform north–south-directed flow field impinging on the Porcupine Mountains Volcanic structure. Our vertical leakage model, in which lateral flow in the Copper Harbor Formation is forced up into the basal Nonesuch by overall aquifer/confining unit thinning, best explains the observed spatial distribution of mineralization at Presque Isle, White Pine, and far along strike (up the Keweenaw and down into North-Eastern Wisconsin).

Grigorita & Brown (2001) recently attributed ore formation at White Pine to thermally driven free convection of oxidized brines within the Copper Harbor Formation because of residual heat from felsic volcanism and associated plutonism. However, the tendency for free convection scales with the thickness and the permeability of the aquifer. The Copper Harbor Formation thins abruptly from about 2 km to about 100 m atop the Porcupine Mountains Volcanic Structure. In the absence of an extremely large thermal anomaly beneath the Porcupine Mountains Volcanic structure, it seems unlikely that convection would nucleate where the aquifer is so thin. As the timing of felsic volcanism significantly predated White Pine ore formation, the residual heat hypothesis of Grigorita & Brown (2001) seems hard to justify.

The results of our study support the following genetic model of stratiform copper mineralization within the Lake Superior basin that, in many respects, represents a synthesis of well-established concepts regarding the source, long-distance transport through the Copper Harbor Formation, and deposition of copper within the basal Nonesuch Formation. In our model, the volcaniclastic Copper Harbor Formation was the ultimate copper source. Oxidation of these sediments during fluvial transport and temporary subaerial exposure converted native copper to cuprite and iron to hematite. Subsequent burial and heating of the Copper Harbor Formation in the presence of seawater or Na–Ca–Cl lacustrine-derived brines generated highly oxidized pore fluids with 10^1–10^2 p.p.m. concentrations of chloride-complexed copper. These ore-forming fluids were driven up-dip (marginward) within the basal aquifer in response to its compaction during deposition of the Freda Formation. Regional-scale (along strike) stratiform mineralization of the basal Nonesuch Formation was produced by stratigraphic thinning of the basal aquifer/confining unit near the basin margins, which induced vertical leakage of compaction-driven discharge into the superjacent marginal lacustrine facies assemblage facies and precipitation of copper in accordance with the well-established overprint model of metal deposition (Brown 1992). The White Pine and Presque Isle ore bodies were formed atop the flanks of the Porcupine Mountains Volcanic structure in response to intense focusing of compaction-driven discharge within the constricted basal aquifer.

Traditional studies of compaction-driven groundwater circulation as a potential ore-forming mechanism focused on environments in which the rapid deposition of thick sequences of low-permeability sediments, i.e. aquitards, generated impressive overpressure (Sharp & Domenico 1976; Bethke 1985). In these studies, the thick aquitard was the source of ore-forming fluid, and its compaction was the basin-scale fluid-impelling mechanism. In our model, aquifer compaction was the delivery system for ore-forming fluids in the Lake Superior basin. We have demonstrated that the transgressive sequence, i.e. the Nonesuch Formation, exerted a first-order control on the hydrodynamic evolution of the Lake Superior basin. Throughout deposition of the Freda Formation, the Nonesuch Formation partitioned the Lake Superior basin's flow regime into a marginward-directed, compaction-driven flow system within the basal aquifer and a basinward-directed, topography-driven flow system in the overlying aquifer (Freda Formation). The transgressive sequence prevented the vertical expulsion of pore fluids from the compacting basal aquifer and focused this discharge laterally to the basin margins. In addition, the Nonesuch Formation sequence formed the necessary chemical sink for cupriferous brines near the basin margins.

The original intention of our study was to extend White's (1971) seminal work by synthesizing new basin-scale geophysical data and high-resolution chronological data with quantitative techniques for modeling basin-scale groundwater circulation. A critical comparison of the two models is thus illuminating. The results of our study support several of White's original hypotheses, including: (i) regional-scale stratiform mineralization and the formation of the White Pine ore body could be ascribed to the marginward (up-dip) migration of pore fluids driven from the compacting basal aquifer (hydrofacies); (ii) the economic grade of copper mineralization at White Pine is attributable to intense structural focusing of lateral discharge within the thinning hydrofacies, regardless of the marginward fluid-impelling mechanism; (iii) a 10-Ma period of ore genesis via compaction of the basal aquifer is reasonable; (iv) the oxidized volcaniclastics of the Copper Harbor Formation formed an ample copper source; and (v) a copper concentration of 50 p.p.m. in the ore-forming fluid is geochemically plausible.

However, of the two hydrologic scenarios he presented to explain stratiform copper mineralization at White Pine, White (1971) favored a topography-driven flow system within the basal aquifer that was fed by meteoric recharge along the north flank of the Lake Superior syncline and discharged south of the present-day ore district. Garven (1985) also argued for this mechanism in the formation of the White Pine ore body. Although such a model can explain the spatial distribution of ore bodies and easily satisfies mass-balance constraints within the ore district, it is inconsistent with both the new data on the structural information of the Lake Superior basin (Cannon *et al.* 1990) and the timing of stratiform mineralization (Ohr 1993). The Freda Formation consists of shallow-dipping, basinward-directed seismic reflectors that are distributed symmetrically about the syncline axis (Allen 1994; Allen *et al.* 1997). Paleocurrent indicators in exposures of the formation are consistent with basinward-discharging fluvial systems (Daniels 1982). On the basis of these stratigraphic data, we infer that the water-table configuration throughout Freda Formation deposition was broadly symmetric about the syncline axis and possessed a gradient that scaled with the depositional slope of the fluvial systems. It follows that the water-table slope was significant only very near the basin margins. Therefore, if stratiform mineralization of the basal Nonesuch Formation was contemporaneous with deposition of the Freda Formation, as is indicated by both relative and absolute dating techniques, then we consider it unlikely that such a water-table configuration could have generated the type of deep, north–south-orientated, cross-basin groundwater circulation within the basal aquifer that White (1971) and Garven (1985) envisioned.

Mountain building during late-stage closure of the Midcontinent Rift System may have generated a basin-wide, water-table geometry of the type generally invoked to explain stratiform mineralization (Garven 1985). However, this far-field compression post-dated stratiform mineralization at White Pine by 20–30 Ma (Bornhorst *et al.* 1988; Cannon 1992; Mauk *et al.* 1992; Ohr 1993), although it may have been responsible for native copper mineralization at White Pine, as proposed by Garven (1985). Furthermore, on the basis of deep seismic reflection data, Cannon *et al.* (1989) suggested that rift inversion was asymmetric, with the maximum displacement along the Keweenaw Fault, which lies to the south of the White Pine ore district (Fig. 1). This pattern of uplift may have generated significant water-table relief, but much of the topography-driven flow would have been northward directed.

CONCLUSION

We present the results of a two-dimensional mathematical model of variable-density groundwater flow and heat transfer that we applied to a cross-section through the Lake Superior syncline of the Midcontinent Rift System. The objective of our study was to determine the relative importance of sediment-compaction, buoyancy, and water-table topography as basin-scale fluid-impelling mechanisms for the transport of cupriferous brines to the White Pine ore district. Combined with recent geophysical, geochemical, and chronological data, our model results suggest that the cupriferous brines responsible for regional-scale stratiform copper mineralization of the basal Nonesuch Formation were derived from the consolidating basal aquifer (Copper Harbor Formation) and migrated marginward (up-dip) within this aquifer in response to compaction caused by the deposition of the overlying Freda Formation. We conclude that stratigraphic thinning of the basal aquifer near the basin margin induced leakage into the lowermost facies of the overlying Nonesuch Formation, where copper was precipitated in response to a change in redox conditions. We attribute the formation of the Presque Isle and White Pine copper mineralization to the intense focusing of compaction-driven discharge, and corresponding amplification of leakage, in response to pronounced thinning of the Copper Harbor Formation (and to a lesser degree, thinning of the Nonesuch Formation) atop the Porcupine Mountain Volcanic Structure. Such fluid focusing represents a primary paradigm for future stratiform copper exploration in the Midcontinent Rift System.

Our model of stratiform copper mineralization satisfies important constraints on the timing of the ore-forming event as well as on the spatial distribution of ore grade. In addition, geochemical modeling indicates that oxidized, chloride-rich pore fluids within the compacting basal aquifer could have transported sufficient copper to satisfy mass-balance constraints within the ore district.

Compaction-driven groundwater circulation generally is disregarded as an effective ore-forming agent. Indeed, we do not advocate sediment compaction as the ubiquitous basin-scale metal-transport mechanism in stratiform ore genesis; that role is better satisfied by topography-driven circulation (Garven & Freeze 1984a,b). Rather, our study indicates that under favorable conditions of intense stratigraphic and structural fluid focusing and high metal solubility, compaction-driven groundwater circulation may be capable of generating economic-grade stratiform mineralization in a layered aquifer/confining unit system. In the case of White Pine, the presence of a transgressive sequence (Nonesuch Formation) was critical to the formation of the ore deposit: in addition to serving as the ultimate sink for copper, the sequence formed an ideal focusing mechanism for fluids driven from the consolidating Copper Harbor Formation. The fundamental characteristics of the White Pine ore body (i.e. an ore-hosting transgressive sequence overlying a redbed aquifer, a continental rift environment, and a diagenetic timing of mineralization) are common to many stratiform copper deposits (Brown 1992), which suggests, perhaps, that the conclusions of our study may apply to other basins.

REFERENCES

Allen DJ (1994) An Integrated Geophysical Investigation of the Midcontinent Rift System: Western Lake Superior, Minnesota, and Wisconsin. PhD Thesis. Purdue University, West Lafayette, Indiana.

Allen DJ, Hinze WJ, Dickas AB, Mudrey MG, Jr (1997) Integrated geophysical modeling of the North American Midcontinent Rift System: new interpretations for western Lake Superior, northwestern Wisconsin, and eastern Minnesota. In: *Middle Proterozoic to Cambrian Rifting, Central North America* (eds Ojakangas RW, Dickas AB, Green JC), pp. 47–72. Special Paper 312. Geological Society of America, GSA, Boulder, CO.

Anderson RR (1997) Keweenawan Supergroup clastic rocks in the Midcontinent Rift of Iowa. In: *Middle Proterozoic to Cambrian Rifting, Central North America* (eds Ojakangas RW, Dickas AB, Green JC), pp. 211–30. Special Paper 312. Geological Society of America, GSA, Boulder, CO.

Appold MS, Garven G (2000) Reactive flow models of ore formation in the Southeast Missouri District. *Economic Geology*, **95**, 1605–26.

Barnes HL (1979) Solubility of ore minerals. In: *Geochemistry of Hydrothermal Ore Deposits* (ed. Barnes HL), pp. 404–60. John Wiley and Sons, New York.

Bethke CM (1985) A numerical model of compaction-driven groundwater flow and heat transfer and its application to the paleohydrology of intracratonic sedimentary basins. *Journal of Geophysical Research*, **90B**, 6817–28.

Bethke CM, Corbet TF (1988) Linear and nonlinear solutions for one-dimensional compaction flow in sedimentary basins. *Water Resources Research*, **24**, 461–7.

Blair CT (1987) Tectonic and hydrologic controls on cyclic alluvial fan, fluvial, and lacustrine rift basin sedimentation, Jurassic-Lowermost Cretaceous Todos Samtos Formation, Chiapa. *Mexico Journal of Sedimentary Petrology*, **57**, 845–62.

Bornhorst TJ (1997) Tectonic context of native copper deposits of the North American Midcontinent Rift System. In: *Middle Proterozoic to Cambrian Rifting, Central North America* (eds Ojakangas RW, Dickas AB, Green JC), pp. 127–36. Special Paper 312. Geological Society of America, GSA, Boulder, CO.

Bornhorst TJ, Paces JB, Grant NK, Obradovich JD, Huber NK (1988) Age of native copper mineralization, Keweenaw Peninsula. *Michigan Economic Geology*, **83**, 619–25.

Brown AC (1971) Zoning in the White Pine copper deposit, Ontonagan County. *Michigan Economic Geology*, **66**, 543–73.

Brown AC (1992) Sediment-hosted stratiform copper deposits. *Geoscience Canada*, **19**, 125–41.

Brown AC (1997) World-class sediment-hosted stratiform copper deposits: characteristics, genetic concepts, and metallotects. *Australian Journal of Earth Sciences*, **44**, 317–28.

Butler BS, Burbank W-S (1929) The copper deposits of Michigan. *US Geological Survey Professional Paper*, **144**, 1–238.

Cannon WF (1992) The Midcontinent rift in the Lake Superior region with emphasis on its geodynamic evolution. *Tectonophysics*, **213**, 41–8.

Cannon WF (1994) Closing of the Midcontinent rift—a far-field effect of Grenvillian compression. *Geology*, **22**, 155–8.

Cannon WF, Cannon WC, Green AG, Hutchinson DR, Lee MW, Milkereit B, Behrendt JC, Halls HC, Green JC, Dickas AB, Morey GB, Sutcliffe R, Spencer C (1989) The Midcontinent rift beneath Lake Superior from GLIMPCE seismic reflection profiling. *Tectonics*, **8**, 305–32.

Cannon WF, Peterman ZE, Sims PK (1990) Structural and isotopic evidence for Middle Proterozoic thrust faulting of Archean and Early Proterozoic rocks near the Gogebic Range, Michigan and Wisconsin (Abstract). In: *Proceedings and Abstracts*, **Vol. 36**, pp. 11–2. Institute on Lake Superior Geology, Thunder Bay, Ontario.

Cathles LM, Smith T (1983) Thermal constraints on the formation of Mississippi-Valley-type lead-zinc deposits and their implications for episodic basin dewatering and deposit genesis. *Economic Geology*, **78**, 983–1002.

Combarnous MA, Bories SA (1975) Hydrothermal convection in saturated porous media. *Advances in Hydroscience*, **10**, 231–307.

Corbet T, Bethke CM (1992) Disequilibrium fluid pressures and groundwater flow in the western Canada sedimentary basins. *Journal of Geophysical Research*, **97**, 7203–17.

Daniels PA, Jr (1982) Upper Precambrian sedimentary rocks: Oronto Group. In: *Geology and Tectonics of the Lake Superior Basin* (eds Wold RJ, Hinze WJ), pp. 107–33. Memoir 156. Geological Society of America, GSA, Boulder, CO.

Davis DW, Paces JB (1990) Time resolution of geological events on the Keweenaw Peninsula and implications for development of the Midcontinent rift system. *Earth and Planetary Science Letters*, **97**, 54–64.

Davis DW, Sutcliffe RH (1985) U-Pb ages from the Nipigon plate and northern Lake Superior. *Geological Society of America Bulletin*, **96**, 1572–9.

De Marsily G (1986) *Quantitative Hydrogeology: Groundwater Hydrology for Engineers*. Academic Press, London.

Duffy CJ, Al-Hassan S (1988) Groundwater circulation in a closed desert basin: Topographic scaling and climatic forcing. *Water Resources Research*, **24**, 1675–88.

Elmore RD (1984) The Copper Harbor Formation: a late Precambrian fining-upward alluvial fan sequence in northern Michigan. *Geological Society of America Bulletin*, **95**, 610–7.

Elmore RD, Milavec GJ, Imbus SW, Engel MH (1989) The Precambrian Nonesuch Formation of the North American midcontinent rift, sedimentology and geochemical aspects of lacustrine deposition. *Precambrian Research*, **43**, 191–213.

Evans DG, Raffensperger JP (1992) On the stream function for variable-density groundwater flow. *Water Resources Research*, **28**, 2141–5.

Garven G (1985) The role of regional fluid flow in the genesis of the Pine Point deposit, western Canada sedimentary basin. *Economic Geology*, **80**, 307–24.

Garven G, Freeze RA (1984a) Theoretical analysis of the role of groundwater flow in the genesis of stratabound ore deposits. Part 1. Mathematical and numerical model. *American Journal of Science*, **284**, 1085–124.

Garven G, Freeze RA (1984b) Theoretical analysis of the role of groundwater flow in the genesis of stratabound ore deposits. Part 2. Quantitative results. *American Journal of Science*, **284**, 1125–56.

Garven G, Appold MS, Toptygina VI, Hazlett TJ (1999) Hydrogeologic modelling of the genesis of carbonate-hosted lead-zinc ores. *Hydrogeology Journal*, **7**, 108–26.

Grigorita A, Brown AC (2001) *Correlation of the White Pine Sediment-Hosted Copper Deposit with an Underlying Resurgent Caldera?*, **Vol. 33** (6), p. 419. Abstracts with Programs, Geological Society of America, GSA, Boulder, CO.

Hanor JS (1979) The sedimentary genesis of hydrothermal fluids. In: *Geochemistry of Hydrothermal Ore Deposits* (ed. Barnes HL), pp. 137–72. John Wiley and Sons, New York.

Hanor JS (1987) *Origin and Migration of Subsurface Sedimentary Brines*. Society of Economic Paleontology and Mineralogy, Short Course 21. SEPM, Tulsa, OK.

Helgeson HC (1969) Thermodynamics of hydrothermal systems at elevated temperatures and pressures. *American Journal of Science*, **267**, 729–804.

Hieshima GB, Pratt LM (1991) Sulfur/carbon ratios and extractable organic matter of the Middle Proterozoic Nonesuch Formation, North American Midcontinent Rift. *Precambrian Research*, **54**, 65–79.

Hinze WJ, Allen DJ, Braile LW, Mariano J (1997) The Mid-continent Rift System: a major Proterozoic continental rift. In: *Middle Proterozoic to Cambrian Rifting, Central North America* (eds Ojakangas RW, Dickas AB, Green JC), pp. 7–35. Special Paper 312. Geological Society of America, GSA, Boulder, CO.

Hubbert MK, Rubey WW (1959) Role of fluid pressure in mechanics of overthrust faulting. Part I. Mechanics of fluid-filled porous solids and its application to overthrust faulting. *Geological Society of America Bulletin*, **70**, 115–66.

Huyakorn PS, Pinder GF (1983) *Computational Methods in Subsurface Flow*. Academic Press, New York.

Johnson JW, Oelkers EH, Helgeson HC (1992) SUPCRT92: a software package for calculating the standard molal thermodynamic properties of mineral gases, aqueous species and reactions from 1 to 5000 bars and 0 to 1000°C. *Computers in Geoscience*, **18**, 899–947.

Johnson RC, Andrews RA, Nelson WS, Suszek T, Sikkila K (1995) *Geology and Mineralization of the White Pine Copper Deposit: 1995*. Copper Range Company, White Pine, MI.

Jowett EC (1986) Genesis of the Kupferschiefer Cu-Ag deposits by convective flow of Rotliegende brines during Triassic rifting. *Economic Geology*, **81**, 1823–37.

Kestin J, Khalifa HE, Correia RJ (1981) Tables of dynamics and kinematic viscosity of NaCl solutions in the temperature range 20–150 °C and the pressure range 0.1–35 MPa. *Journal of Physical Chemistry Reference Data*, **10**, 71–87.

Mauk JL (1993) Geological and Geochemical Investigations of the White Pine Sediment-Hosted Stratiform Copper Deposit, Ontonagon County, Michigan. PhD Thesis. The University of Michigan, Ann Arbor.

Mauk JL, Kelly WC, van der Pluijm BA, Seasor RW (1992) Relations between deformation and sediment-hosted copper mineralization: evidence from the White Pine part of the Midcontinent rift system. *Geology*, **20**, 427–30.

McKenzie DP (1978) Some remarks on the development of sedimentary basins. *Earth and Planetary Science Letters*, **40**, 25–32.

Morey GB (1974) Cyclic sedimentation of the Solor Church Formation (upper Precambrian, Keweenawan), southeastern Minnesota. *Journal of Sedimentary Petrology*, **44**, 872–84.

Neuzil CE (1994) How permeable are clays and shales? *Water Resources Research*, **30**, 145–50.

Nield DA, Bejan A (1992) *Convection in Porous Media*. Springer–Verlag, New York.

Ohr M (1993) Geochronology of Diagenesis and Low-Grade Metamorphism in Pelites. PhD Thesis. The University of Michigan, Ann Arbor.

Palmer HC, Davis DW (1987) Paleomagnetism and U-Pb geochronology of Michipicoten Island: precise calibration of the Keweenawan polar wander track. *Precambrian Research*, **37**, 157–71.

Person MA, Garven G (1994) A sensitivity study of the driving forces on fluid flow during continental-rift basin evolution. *Geological Society of America Bulletin*, **106**, 461–75.

Price KL, McDowell SD (1993) Illite / smectite geothermometry of the Proterozoic Oronto Group, Midcontinent rift system. *Clays and Clay Minerals*, **41**, 134–47.

Price KL, Huntoon JE, McDowell SD (1996) Thermal history of the 1.1-Ga Nonesuch Formation, North American Mid-continent rift, White Pine. *Michigan American Association of Petroleum Geologists Bulletin*, **80**, 1–15.

Raffensperger JP, Garven G (1995) The formation of unconformity-type uranium ore deposits. Part 1. Coupled groundwater flow and heat transport modeling. *American Journal of Science*, **295**, 581–630.

Riahi N (1983) Nonlinear convection in a porous layer with finite conducting boundaries. *Journal of Fluid Mechanics*, **129**, 153–71.

Rose AW (1976) The effect of cuprous chloride complexes in the origin of red-bed copper and related deposits. *Economic Geology*, **71**, 1036–1048.

Rose AW (1989) Mobility of copper and other heavy metals in sedimentary environments. In: *Sediment-Hosted Stratiform Copper Deposits* (eds Boyle RW, Brown AC, Jefferson CW, Jowett EC, Kirkham RV), pp. 257–67. Special Paper 36. Geological Society of Canada, Toronto, ON, Canada.

Sales RH (1959) The White Pine copper deposit—a discussion. *Economic Geology*, **54**, 947–50.

Scofield N (1976) Mineral Chemistry Applied to Interrelated Albitization, Pumpellyitization, and Native Copper Redistribution in Some Portage Lake basalts. Michigan. Unpublished PhD Dissertation. Michigan Technological University, Houghton, Michigan.

Sharp JM, Jr (1978) Energy and momentum transport model of the Ouachita basin and its possible impact on formation of economic mineral deposits. *Economic Geology*, **73**, 1057–68.

Sharp JM, Jr, Domenico PA (1976) Energy transport in thick sequences of compacting sediment. *Geological Society of America Bulletin*, **87**, 390–400.

Suszek T (1997) Petrography and sedimentation of the Middle Proterozoic (Keweenawan) Nonesuch Formation, western Lake Superior region, Midcontinent Rift System. In: *Middle Proterozoic to Cambrian Rifting, Central North America* (eds Ojakangas RW, Dickas AB, Green JC), pp. 195–210. Special Paper 312. Geological Society of America, GSA, Boulder, CO.

Sverjensky DA (1987) The role of migrating oil-field brines in the formation of sediment-hosted Cu-rich deposits. *Economic Geology*, **82**, 1130–41.

Tóth J (1963) A theoretical analysis of groundwater flow in small drainage basins. *Journal of Geophysical Research*, **68**, 4795–812.

Van Schmus WR (1992) Tectonic setting of the Midcontinent rift system. *Tectonophysics*, **213**, 1–15.

White WS (1968) The native copper deposits of northern Michigan. In: *Ore Deposits of the United States, 1933–1967* (ed. Ridge JD), pp. 303–25. American Institute of Mining, Metallurgical, and Petroleum Engineers, New York, NY.

White WS (1971) A paleohydrologic model for mineralization of the White Pine copper deposit, northern Michigan. *Economic Geology*, **66**, 1–13.

White WS, Wright JC (1954) The White Pine copper deposit, Ontonagon County. *Michigan Economic Geology*, **49**, 675–716.

White WS, Wright JC (1966) Sulfide mineral zoning in the basal Nonesuch Shale, northern Michigan. *Economic Geology*, **61**, 1171–90.

Witzke BJ (1990) General stratigraphy of the Phanerozoic and Keweenawan sequence, M.G. Eischeid #1 drillhole, Carrol Co., Iowa. In: *The Amoco M.G. Eischeid #1 Deep Petroleum Test, Carrol County, Iowa* (ed. Anderson RR), pp. 39–57. Special Report Series no. 2. Iowa Geological Survey, Iowa City, IA.

Wolery TJ (1992) *Calculation of Chemical Equilibrium Between Aqueous Solution and Minerals: the EQ3/6 Software Package*. United States Department of Energy, Lawrence Livermore Laboratory, Livermore.

Wolff RG, Huber NK (1973) *The Copper Harbour Conglomerate (Middle Keweenawan) on Isle Royale, Michigan, and its Regional Implications.* US Geological Survey, Reston, VA.

Wood JA, Hewett TA (1984) Reservoir diagenesis and convective fluid flow. In: *Clastic Diagenesis* (eds Surdam RC, McDonald DA), pp. 99–110. Memoir 37. American Association of Petroleum Geologists, Tulsa, OK.

Zartman RE, Nicholson SW, Cannon WF, Morey GB (1997) U-Th-Pb zircon ages of some Keweenawan Supergroup rocks from the south shore of Lake Superior. *Candian Journal of Earth Sciences*, **34**, 549–61.

APPENDIX: MATHEMATICAL MODEL

We adopt the methodology of Garven & Freeze (1984a,b) and Person & Garven (1994) for representing two-dimensional groundwater circulation and heat transfer in evolving sedimentary basins. A cross-sectional representation of the paleoflow field is justified by the large ratio of longitudinal (strike-parallel) to transverse length scales that characterizes the curvilinear Lake Superior syncline (Fig. 1). We describe variable-density groundwater circulation in a compacting porous medium with a head-based governing equation that is a combination of fluid-phase mass conservation:

$$-\nabla \cdot \rho_f \vec{q} = S_s \rho_f \left[\frac{\partial h}{\partial t} + \frac{\rho_b - \rho_f}{\rho_f} \frac{\partial L}{\partial t} \right] + \phi \rho_f \alpha_T \frac{\partial T}{\partial t} \qquad (A.1)$$

and Darcy's Law (see Table 1 for definition of symbols):

$$\vec{q} = (q_x, q_z) = -\frac{\rho_0 g}{\mu_f} [k] \left[\nabla h + \frac{\rho_f - \rho_0}{\rho_0} \nabla z \right] \qquad (A.2)$$

In a vertically consolidating medium, conservation of the solid phase is (Bethke & Corbet 1988):

$$\frac{\partial v_s}{\partial z} = \frac{1}{1-\phi} \frac{\partial \phi}{\partial t} \qquad (A.3)$$

Porosity decays exponentially with increasing effective stress (Hubbert & Rubey 1959):

$$\phi = \phi_0 \exp\left[-\frac{b \sigma_e}{g(1-\phi)} \right] \qquad (A.4)$$

Both permeability and specific storage are functions of porosity (Bethke 1985; Bethke & Corbet 1988; Neuzil 1994):

$$\log(k_x/k_0) = c_1 \phi + c_0 \qquad (A.5)$$

$$S_s = \frac{\rho_f}{(\rho_b - \rho_f)} \frac{b\phi}{(1-\phi)} \qquad (A.6)$$

We describe heat transfer via conduction and groundwater advection with a temperature-based continuity equation:

$$[\rho_f \phi c_f + \rho_s (1-\phi) c_s] \frac{\partial T}{\partial t} + \frac{\rho_f h_f}{(1-\phi)} \frac{\partial \phi}{\partial t} = \nabla \cdot [\lambda] \nabla T - \rho_f c_f \vec{q} \cdot \nabla T \qquad (A.7)$$

Table 1 Notation (dimensions: M, mass; L, length; T, time; θ, temperature).

Symbol	Dimensions	Description
α_T	θ^{-1}	Thermal expansivity of porous medium
b	LT^2M^{-1}	Porous medium consolidation coefficient
β_{WT}	L^{-1}	Water-table spatial decay parameter
C	0	Pore-fluid salinity (mass fraction)
χ	0	Fluid–rock ratio
χ_∞	0	Maximum fluid–rock ratio
C_{Cu}	0	Local efficiency of copper precipitation
C_{max}	0	Maximum pore-fluid concentration
c_0, c_1	0	Empirical coefficients $k^x - \phi$
c_f, c_s	$L^2T^{-2}\,\theta^{-1}$	Fluid and solid specific heat capacities
d	L	Depth below land surface
$[D]$	L^2T^{-1}	Hydrodynamic dispersion tensor
d_{max}	L	Maximum depth of pore-fluid salinity variation
ε	0	Local efficiency of copper precipitation
ϕ, ϕ_0, ϕ_r	0	Porosity, depositional porosity, representative porosity for the Nonesuch marginal lacustrine facies
g	LT^{-2}	Gravitational acceleration
h	L	Hydraulic head (freshwater equivalent)
H	L	Aquifer thickness
η	0	Log permeability ratio; $\eta = \log(k_{CHF}/k_{LFA})$
h_f	L^2T^{-2}	Fluid specific enthalpy
h_{WT}	L	Prescribed water-table configuration
h_{FH}	L	Water table at alluvial fan head
$[I]$	0	Identity tensor
J_z	MT^{-2}	Basal heat flux
$[k]$	L^2	Permeability tensor
k_0	L^2	Reference permeability
k_x, k_z	L^2	Bedding – parallel and perpendicular permeabilities
k_{CHF}, k_{LFA}, k_{MLFA}	L^2	Permeability of Copper Harbor Formation (CHF), Lacustrine Facies (LFA), and Marginal Lacustrine Facies (MLFA)
L	L	Sediment thickness
λ_f, λ_s	$MLT^{-3}\theta^{-1}$	Fluid and solid thermal conductivities
$[\lambda]$	$MLT^{-3}\theta^{-1}$	Thermal conduction–dispersion tensor
μ_f	$ML^{-1}T^{-1}$	Fluid viscosity
m_{Cu}	ML^{-3}	Metal (copper) mass per unit rock volume
$q\rightarrow$; q_x, q_z	LT^{-1}	Darcy Flux vector; Components of Darcy flux in x- and z-directions
Q_z	L	Time-integrated leakage
$Q_{z\infty}$	L	Maximum time-integrated leakage
Ra	0	Rayleigh number
ρ_0	ML^{-3}	Reference fluid density
ρ_f, ρ_s	ML^{-3}	Fluid and solid densities, respectively
σ_e	$L^{-1}T^{-2}M$	Effective stress on porous medium
S_s	L^{-1}	Specific storage
S_{WT}	0	Linear water-table slope
t	T	Time
T	θ	Temperature of porous medium
v_s	LT^{-1}	Vertical velocity of solid phase
V_u	L^3	Unit volume of rock
x_{FH}	L	Lateral position of alluvial fan head
Ψ	ML^2T^{-1}	Stream Functions
ξ	0	Log permeability ratio; $\xi = \log(k_{CHF}/k_{MLFA})$
z	L	Elevation above datum

Note that we ignore heat production by radiogenic decay of the volcaniclastic basin fill. Following Combarnous & Bories (1975) and Garven & Freeze (1984a), we expand the conduction–dispersion tensor in terms of the solid and liquid

thermal conductivities and the hydrodynamic dispersion tensor:

$$[\lambda] = \lambda_{\mathrm{f}}^{\phi}\lambda_{\mathrm{s}}^{1-\phi}[I] + \rho_{\mathrm{f}}c_{\mathrm{f}}[D] \tag{A.8}$$

We couple the governing equations for groundwater circulation and heat transfer, i.e. equations 1, 2, and 7, with second-order polynomial expressions that relate fluid density to temperature and pressure (Kestin *et al.* 1981). Representative values of rock and fluid properties are compiled in Garven & Freeze (1984a), De Marsily 1986), and Bethke & Corbet (1988).

We also present simulations of paleoflow after basin formation, but prior to tectonic inversion, using a coupled model of steady-state stream-function-based groundwater circulation and heat transfer that is described in Evans & Raffensperger (1992). This approach provides advantages in quantifying and visualizing strongly density-dependent groundwater circulation. The discharge vector and governing equation for groundwater circulation are:

$$\vec{q} = (q_x, q_z) = \frac{1}{\rho_f}\left(-\frac{\partial\Psi}{\partial z}, \frac{\partial\Psi}{\partial x}\right) \tag{A.9}$$

$$\nabla \cdot \frac{[k]}{|[k]|}\frac{\mu_{\mathrm{f}}}{\rho_{\mathrm{f}}\rho_0 g}\nabla\Psi = -\frac{\partial}{\partial x}\left(\frac{\rho_{\mathrm{f}} - \rho_0}{\rho_0}\right) \tag{A.10}$$

We use a Galerkin-based finite element formulation to obtain approximate solutions to the governing equations for groundwater circulation and heat transfer in both the transient and steady-state models. We solve the one-dimensional solid-phase conservation equation via a finite-difference technique (e.g. Huyakorn & Pinder 1983). In the transient model, basin growth requires dynamic re-meshing of the solution domain throughout the simulation (e.g. Fig. 4B,C). Details of the numerical solution approach are contained in Person *et al.* (2000).